

Rényi Divergence Variational Inference

Yingzhen Li
University of Cambridge
Cambridge, CB2 1PZ, UK
y1494@cam.ac.uk

Richard E. Turner
University of Cambridge
Cambridge, CB2 1PZ, UK
ret26@cam.ac.uk

Abstract

This paper introduces the *variational Rényi bound (VR)* that extends traditional variational inference to Rényi's α -divergences. This new family of variational methods unifies a number of existing approaches, and enables a smooth interpolation from the evidence lower-bound to the log marginal likelihood that is controlled by the value of α that parametrises the divergence. The reparameterization trick, Monte Carlo approximation and stochastic optimisation methods are deployed to obtain a unified framework for optimisation. We further consider negative α values and propose a novel variational inference method as a new special case in the proposed framework. Experiments on Bayesian neural networks and variational auto-encoders demonstrate the wide applicability of the VR bound.

1 Introduction

Approximate inference is at the core of modern probabilistic modelling. It is primarily used for approximating intractable posterior distributions and log-likelihood functions. This paper focuses on optimisation-based approximate inference algorithms, popular examples of which include variational inference (VI), variational Bayes (VB) [1, 2] and expectation propagation (EP) [3, 4]. Historically, VI has received more attention compared to other approaches, mainly because VI has elegant and potentially useful theoretical properties such as the fact that it maximises the negative *variational free-energy* (VFE) that is a lower-bound of the log-model evidence. Such a lower-bound can serve as a surrogate to both maximum likelihood estimation (MLE) of the hyper-parameters and posterior approximation by Kullback-Leibler (KL) divergence minimisation.

Recent advances of approximate inference follows three major trends. First, scalable methods, e.g. stochastic variational inference (SVI) [5] and stochastic expectation propagation (SEP) [6, 7], have been developed for datasets comprising millions of datapoints. Recent approaches [8, 9, 10] have also applied variational methods to coordinate distributed inference on sub-datasets. Second, Monte Carlo (MC) methods and black-box inference techniques have been deployed to extend the applicability of variational methods to previously intractable models and complex posterior approximations. These methods include MC-VI [11, 12] and [13] for EP. They all proposed ascending the Monte Carlo approximated variational bounds to the log-likelihood using noisy gradients computed with automatic differentiation tools. Third, tighter variational lower-bounds have been proposed for (approximate) MLE. The importance weighted auto-encoder (IWAE) [14] improved upon the variational auto-encoder (VAE) [15, 16] framework, by providing tighter lower-bound approximations to the log-likelihood using importance sampling. These developments are rather separated and little work has been done to understand their connections.

In this paper we try to provide a unified framework that encompasses a number of recent advances of variational methods, and we hope our effort could potentially motivate new algorithms in the future. This is done by extending traditional VI to Rényi's α -divergence [17], a rich family that includes many well-known divergences as special cases. After reviewing useful properties of Rényi divergences and the VI framework, we make the following contributions:

- We introduce the *variational Rényi bound (VR)* as an extension of VI/VB. Through developments we connect to existing approaches, including VI/VB, VAE, IWAE [14], SEP [6] and black-box alpha (BB- α) [13], to show the richness of this new family of variational methods.
- We develop an optimisation framework for the VR bound. An analysis of the bias introduced by stochastic approximation is also provided with theoretical guarantees and empirical results.

Table 1: Special cases in the Rényi divergence family.

α	Definition	Notes
$\alpha \rightarrow 1$	$\int p(\boldsymbol{\theta}) \log \frac{p(\boldsymbol{\theta})}{q(\boldsymbol{\theta})} d\boldsymbol{\theta}$	<i>Kullback-Leibler (KL) divergence</i> , used in VI (KL[q p]) and EP (KL[p q])
$\alpha = 0.5$	$-2 \log(1 - \text{Hel}^2[p q])$	proportional to squared <i>Hellinger distance</i>
$\alpha \rightarrow 0$	$-\log \int_{p(\boldsymbol{\theta}) > 0} q(\boldsymbol{\theta}) d\boldsymbol{\theta}$	zero when $\text{supp}(p) \subseteq \text{supp}(q)$ (not a divergence)
$\alpha = 2$	$\log(1 + \chi^2[p q])$	proportional to the χ^2 -divergence
$\alpha \rightarrow +\infty$	$\log \max_{\boldsymbol{\theta} \in \Theta} \frac{p(\boldsymbol{\theta})}{q(\boldsymbol{\theta})}$	<i>worst-case regret</i> in <i>minimum description length principle</i> [21]

- We propose a novel approximate inference algorithm called *VR-max* as a new special case. Evaluations on VAEs and Bayesian neural networks show that this new method is often comparable to or better than a number of the state-of-the-art variational methods.

2 Background

This section reviews Rényi’s α -divergence and variational inference upon which the new framework is based. Note that there exist other α -divergence definitions including [18, 19] (see appendix). However we mainly focus on Rényi’s definition in order to derive a new class of variational lower-bounds.

2.1 Rényi’s α -divergence

We first review Rényi’s α -divergence [17, 20]. Rényi’s α -divergence, defined on $\alpha > 0, \alpha \neq 1$, measures the “closeness” of two distributions p and q on a random variable $\boldsymbol{\theta} \in \Theta$:

$$D_\alpha[p||q] = \frac{1}{\alpha - 1} \log \int p(\boldsymbol{\theta})^\alpha q(\boldsymbol{\theta})^{1-\alpha} d\boldsymbol{\theta}. \quad (1)$$

For discrete random variables the integration is replaced by summation. One can extend the definition to $\alpha = 0, 1, +\infty$ by continuity in α . In particular, when $\alpha \rightarrow 1$ it recovers the Kullback-Leibler (KL) divergence that plays a crucial role in machine learning and information theory. We also include some special cases in Table 1. A critical question to ask here is how to choose a divergence in this rich family to obtain optimal solution for a particular application, which is still an open question in active research.

In [20] the definition (1) is also extended to $\alpha \leq 0$, although in that case it is non-positive and is thus no longer a valid divergence measure. The method proposed in this work also considers negative α values, and we include from [20] some useful properties for forthcoming derivations.

Proposition 1. *Rényi’s α -divergence definition, extended to negative α , is **continuous** and **non-decreasing** on $\alpha \in \{\alpha : -\infty < D_\alpha < +\infty\}$.*

Proposition 2. *(Skew symmetry) For $\alpha \neq 0, 1$, $D_\alpha[p||q] = \frac{\alpha}{1-\alpha} D_{1-\alpha}[q||p]$. This implies $D_\alpha[p||q] \leq 0$ for $\alpha < 0$. For the limiting case $D_{-\infty}[p||q] = -D_{+\infty}[q||p]$.*

2.2 Variational inference

Next we review the variational inference algorithm [1, 2] using posterior approximation as a running example. Consider observing a dataset of N i.i.d. samples $\mathcal{D} = \{\mathbf{x}_n\}_{n=1}^N$ from a probabilistic model $p(\mathbf{x}|\boldsymbol{\theta})$ parametrised by a random variable $\boldsymbol{\theta}$ that is drawn from a prior $p_0(\boldsymbol{\theta})$. Bayesian inference involves computing the posterior distribution of the parameters given the data,

$$p(\boldsymbol{\theta}|\mathcal{D}, \boldsymbol{\varphi}) = \frac{p(\boldsymbol{\theta}, \mathcal{D}|\boldsymbol{\varphi})}{p(\mathcal{D}|\boldsymbol{\varphi})} = \frac{p_0(\boldsymbol{\theta}|\boldsymbol{\varphi}) \prod_{n=1}^N p(\mathbf{x}_n|\boldsymbol{\theta}, \boldsymbol{\varphi})}{p(\mathcal{D}|\boldsymbol{\varphi})}, \quad (2)$$

where $p(\mathcal{D}|\boldsymbol{\varphi}) = \int p_0(\boldsymbol{\theta}|\boldsymbol{\varphi}) \prod_{n=1}^N p(\mathbf{x}_n|\boldsymbol{\theta}, \boldsymbol{\varphi}) d\boldsymbol{\theta}$ is often called marginal likelihood or model evidence. The hyper-parameters of the model is denoted as $\boldsymbol{\varphi}$ which might be omitted to reduce notational clutter. For

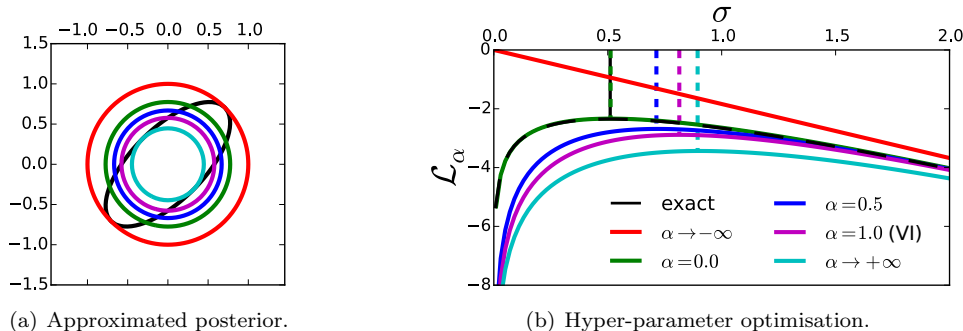


Figure 1: Mean-field approximation for Bayesian linear regression. In this case $\varphi = \sigma$ the observation noise variance. The bound is tight as $\sigma \rightarrow +\infty$, biasing the VI solution to large σ s.

many powerful models the true posterior is typically intractable, and approximate inference introduces an approximation $q(\boldsymbol{\theta})$ in some tractable distribution family \mathcal{Q} to the true posterior. One way to obtain this approximation is to minimise the KL divergence $\text{KL}[q(\boldsymbol{\theta})||p(\boldsymbol{\theta}|\mathcal{D})]$, which is also intractable due to the difficult term $p(\mathcal{D})$. Variational inference (VI) sidesteps this difficulty by considering an equivalent optimisation problem that maximises the *variational lower-bound*:

$$\mathcal{L}_{VI}(q; \mathcal{D}, \varphi) = \log p(\mathcal{D}|\varphi) - \text{KL}[q(\boldsymbol{\theta})||p(\boldsymbol{\theta}|\mathcal{D}, \varphi)] = \mathbb{E}_q \left[\log \frac{p(\boldsymbol{\theta}, \mathcal{D}|\varphi)}{q(\boldsymbol{\theta})} \right]. \quad (3)$$

The variational lower-bound can also be used to optimise the hyper-parameters φ .

To illustrate the approximation quality of VI we present a mean-field approximation example to Bayesian linear regression in Figure 1(a) (in magenta). Readers are referred to the appendix for details, but essentially a factorised Gaussian approximation is fitted to the true posterior, which is a correlated Gaussian in this case. The approximation recovers the posterior mean correctly, but is over-confident, under-estimating the uncertainty. Moreover, as \mathcal{L}_{VI} is the difference between the marginal likelihood and the KL divergence, hyper-parameter optimisation can be biased away from the exact MLE solution towards the region where the KL term is small [22] (see Figure 1(b)).

3 Variational Rényi bound

Recall from Section 2.1 that the family of Rényi divergences includes the KL divergence. Perhaps variational free-energy approaches can be generalised to the Rényi case? Consider approximating the true posterior $p(\boldsymbol{\theta}|\mathcal{D})$ by minimizing Rényi's α -divergence $D_\alpha[q(\boldsymbol{\theta})||p(\boldsymbol{\theta}|\mathcal{D})]$ for some selected $\alpha \geq 0$. Now we verify the equivalent optimization problem $\max_{q \in \mathcal{Q}} \log p(\mathcal{D}) - D_\alpha[q(\boldsymbol{\theta})||p(\boldsymbol{\theta}|\mathcal{D})]$, and when $\alpha \neq 1$, the objective can be rewritten as

$$\mathcal{L}_\alpha(q; \mathcal{D}) := \frac{1}{1-\alpha} \log \mathbb{E}_q \left[\left(\frac{p(\boldsymbol{\theta}, \mathcal{D})}{q(\boldsymbol{\theta})} \right)^{1-\alpha} \right]. \quad (4)$$

We name this new objective the *variational Rényi (VR) bound*. Importantly we also extend the above definition to $\alpha < 0$, and the following theorem is a direct result of Proposition 1.

Theorem 1. *The objective $\mathcal{L}_\alpha(q; \mathcal{D})$ is **continuous** and **non-increasing** on $\alpha \in \{\alpha : |\mathcal{L}_\alpha| < +\infty\}$. Especially for all $0 \leq \alpha_1 < 1$ and $\alpha_2 \leq 0$,*

$$\mathcal{L}_{VI}(q; \mathcal{D}) = \lim_{\alpha \rightarrow 1} \mathcal{L}_\alpha(q; \mathcal{D}) \leq \mathcal{L}_{\alpha_1}(q; \mathcal{D}) \leq \mathcal{L}_0(q; \mathcal{D}) \leq \mathcal{L}_{\alpha_2}(q; \mathcal{D}).$$

Also $\mathcal{L}_0(q; \mathcal{D}) = \log p(\mathcal{D})$ if and only if the support $\text{supp}(p(\boldsymbol{\theta}|\mathcal{D})) \subseteq \text{supp}(q(\boldsymbol{\theta}))$.

The above theorem indicates that VR bound can be useful for model selection by sandwiching the marginal likelihood with bounds computed using positive and negative α values. In particular \mathcal{L}_0 returns the exact $\log p(\mathcal{D})$ under the mild assumption that q is supported where the true posterior is supported.

This assumption holds for many commonly used distributions, e.g. Gaussians are supported on the entire space, and in the following we assume that this condition is satisfied.

Choosing different alpha values allows the approximation to balance between mode-seeking ($\alpha \rightarrow +\infty$) and mass-covering ($\alpha \rightarrow -\infty$) behaviour. This is illustrated by the Bayesian linear regression example, again in Figure 1(a). First notice that $\alpha \rightarrow +\infty$ (in cyan) still returns uncertainty estimates (although more over-confident than VI) which is different from maximum a posterior (MAP). Second, setting $\alpha = 0.0$ (in green) returns $q(\boldsymbol{\theta}) = \prod_i p(\theta_i|\mathcal{D})$ and an exact estimation of $\log p(\mathcal{D})$ (Figure 1(b)). Also the approximate MLE is less biased for $\alpha = 0.5$ (in blue) since now the tightness of the bound is less hyper-parameter dependent.

4 The VR bound optimisation framework

This section addresses several issues of the VR bound optimisation by proposing further approximations. First when $\alpha \neq 1$, the VR bound is usually just as intractable as the marginal likelihood for many useful models. However Monte Carlo (MC) approximation is applied here to extend the set of models that can be handled. The resulting method can be applied to any model that MC-VI [11, 12] is applied to. Second, Theorem 1 suggests that the VR bound is to be minimised when $\alpha < 0$, which performs disastrously in MLE context. As we shall see, this issue is solved also by the MC approximation under certain conditions. Third, a mini-batch training method is developed for large-scale datasets in the posterior approximation context. Hence the proposed optimisation framework of the VR bound enables tractable application to the same class of models as SVI.

4.1 Monte Carlo approximation of the VR bound

Consider learning a latent variable model with MLE as a running example, where the model is specified by a conditional distribution $p(\mathbf{x}|\mathbf{h}; \boldsymbol{\varphi})$ and a prior $p(\mathbf{h}; \boldsymbol{\varphi})$ on the latent variables \mathbf{h} . Examples include the variational auto-encoder (VAE) [15, 16] that parametrises the conditional distribution with a (deep) neural network. MLE requires $\log p(\mathbf{x})$ which is obtained by marginalising out \mathbf{h} and is often intractable, so the VR bound is considered as an alternative optimisation objective. However instead of exact computation, a simple Monte Carlo (MC) method is deployed, which uses finite samples $\mathbf{h}_k \sim q(\mathbf{h}|\mathbf{x}), k = 1, \dots, K$ to approximate $\mathcal{L}_\alpha \approx \hat{\mathcal{L}}_{\alpha, K}$:

$$\hat{\mathcal{L}}_{\alpha, K}(q; \mathbf{x}) = \frac{1}{1 - \alpha} \log \frac{1}{K} \sum_{k=1}^K \left[\left(\frac{p(\mathbf{h}_k, \mathbf{x})}{q(\mathbf{h}_k|\mathbf{x})} \right)^{1-\alpha} \right]. \quad (5)$$

The importance weighted auto-encoder (IWAE) [14] is a special case of this framework applied to the VAE with $\alpha = 0$ and $K < +\infty$. But unlike traditional VI, here the MC approximation is biased. Fortunately we can bound the bias by the following theorems proved in the appendix.

Theorem 2. $\mathbb{E}_{\{\mathbf{h}_k\}_{k=1}^K} [\hat{\mathcal{L}}_{\alpha, K}(q; \mathbf{x})]$ as a function of $\alpha \in \{\alpha : |\mathcal{L}_\alpha| < +\infty\}$ and $K \geq 1$ is:

- 1) **non-decreasing** in K for fixed $\alpha \leq 1$, and **non-increasing** in K for fixed $\alpha \geq 1$;
- 2) $\mathbb{E}_{\{\mathbf{h}_k\}_{k=1}^K} [\hat{\mathcal{L}}_{\alpha, K}(q; \mathbf{x})] \rightarrow \mathcal{L}_\alpha$ when $|\mathcal{L}_\alpha| < +\infty$;
- 3) **continuous** and **non-increasing** in α with fixed K .

Corollary 1. Given $1 \leq K < +\infty$, either $\mathbb{E}_{\{\mathbf{h}_k\}_{k=1}^K} [\hat{\mathcal{L}}_{\alpha, K}(q; \mathbf{x})] \leq \log p(\mathbf{x})$ for all α , or there exists $\alpha_K \leq 0$ such that $\mathbb{E}_{\{\mathbf{h}_k\}_{k=1}^K} [\hat{\mathcal{L}}_{\alpha_K, K}(q; \mathbf{x})] = \log p(\mathbf{x})$ and $\mathbb{E}_{\{\mathbf{h}_k\}_{k=1}^K} [\hat{\mathcal{L}}_{\alpha, K}(q; \mathbf{x})] > \log p(\mathbf{x})$ for all $\alpha < \alpha_K$. Also α_K is **non-decreasing** in K , with $\lim_{K \rightarrow 1} \alpha_K = -\infty$ and $\lim_{K \rightarrow +\infty} \alpha_K = 0$.

The intuition behind the theorems is visualised in Figure 2(a). By definition, the exact VR bound is a lower-bound or upper-bound of $\log p(\mathcal{D})$ when $\alpha > 0$ or $\alpha < 0$, respectively (red lines). However for $\alpha \leq 1$ the MC approximation $\mathbb{E}[\hat{\mathcal{L}}_{\alpha, K}]$ under-estimates the exact VR bound \mathcal{L}_α (blue dashed lines), where the approximation quality can be improved using more samples (the blue dashed arrow). Thus for finite samples, negative alpha values ($\alpha_2 < 0$) can be used to improve the accuracy of the approximation (see the red arrow between the two blue dashed lines). Figure 2(b) shows an empirical evaluation by computing the exact and the MC approximation of the Rényi divergences. In this example p, q are 2-D Gaussian distributions with $\boldsymbol{\mu}_p = [0, 0]$, $\boldsymbol{\mu}_q = [1, 1]$ and $\boldsymbol{\Sigma}_p = \boldsymbol{\Sigma}_q = \mathbf{I}$. The sampling procedure is repeated 200 times to estimate the expectation. Clearly for $K = 1$ it is equivalent to an unbiased

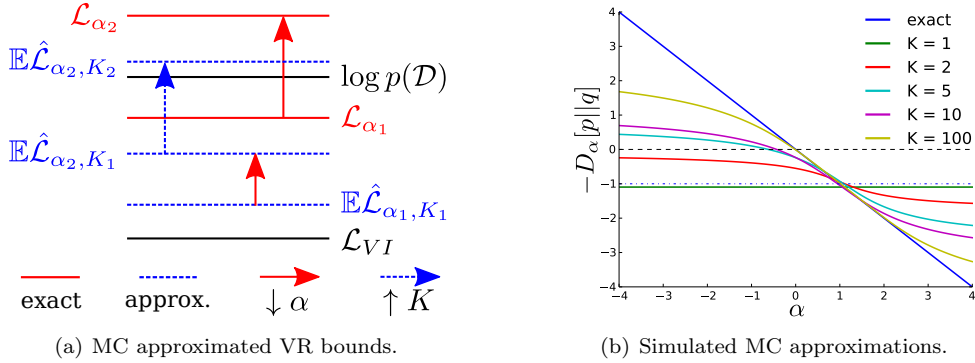


Figure 2: (a) An illustration for the bounding properties of MC approximations to the VR bounds. Here $\alpha_2 < 0 < \alpha_1 < 1$ and $1 < K_1 < K_2 < +\infty$. (b) The bias of the MC approximation on (negative) Rényi divergences. Best viewed in colour.

stochastic estimate of the KL-divergence for all α (even now the estimation is biased for D_α). For $K > 1$ and $\alpha < 1$, the MC approximation under-estimates the VR bound, and the bias decreases when increasing K . For $\alpha > 1$ the inequality is reversed, also as predicted by the theorems.

4.2 Unified implementation with the reparameterization trick

Readers may have noticed that \mathcal{L}_{VI} has a different form compared to \mathcal{L}_α with $\alpha \neq 1$. In this section we show how to unify the implementation for all finite α settings using the *reparameterization trick* [15] as an example. This trick assumes the existence of the mapping $\boldsymbol{\theta} = g_\phi(\boldsymbol{\epsilon})$, where the distribution of the noise term $\boldsymbol{\epsilon}$ satisfies $q(\boldsymbol{\theta})d\boldsymbol{\theta} = p(\boldsymbol{\epsilon})d\boldsymbol{\epsilon}$. Then the expectation of a function $F(\boldsymbol{\theta})$ over distribution $q(\boldsymbol{\theta})$ can be computed as $\mathbb{E}_{q(\boldsymbol{\theta})}[F(\boldsymbol{\theta})] = \mathbb{E}_{p(\boldsymbol{\epsilon})}[F(g_\phi(\boldsymbol{\epsilon}))]$. One prevalent example is the Gaussian reparameterization: $\boldsymbol{\theta} \sim \mathcal{N}(\boldsymbol{\mu}, \Sigma) \Rightarrow \boldsymbol{\theta} = \boldsymbol{\mu} + \Sigma^{\frac{1}{2}}\boldsymbol{\epsilon}, \boldsymbol{\epsilon} \sim \mathcal{N}(\mathbf{0}, I)$. Now we apply the reparameterization trick to the VR bound

$$\mathcal{L}_\alpha(q_\phi; \mathbf{x}) = \frac{1}{1-\alpha} \log \mathbb{E}_\epsilon \left[\left(\frac{p(g_\phi(\boldsymbol{\epsilon}), \mathbf{x})}{q(g_\phi(\boldsymbol{\epsilon}))} \right)^{1-\alpha} \right]. \quad (6)$$

Then the gradient of the VR bound w.r.t. ϕ is (similar for φ , see appendix for derivation)

$$\nabla_\phi \mathcal{L}_\alpha(q_\phi; \mathbf{x}) = \mathbb{E}_\epsilon \left[w_\alpha(\boldsymbol{\epsilon}; \phi, \mathbf{x}) \nabla_\phi \log \frac{p(g_\phi(\boldsymbol{\epsilon}), \mathbf{x})}{q(g_\phi(\boldsymbol{\epsilon}))} \right], \quad (7)$$

where $w_\alpha(\boldsymbol{\epsilon}; \phi, \mathbf{x}) = \left(\frac{p(g_\phi(\boldsymbol{\epsilon}), \mathbf{x})}{q(g_\phi(\boldsymbol{\epsilon}))} \right)^{1-\alpha} / \mathbb{E}_\epsilon \left[\left(\frac{p(g_\phi(\boldsymbol{\epsilon}), \mathbf{x})}{q(g_\phi(\boldsymbol{\epsilon}))} \right)^{1-\alpha} \right]$ denotes the normalised importance weight.

One can show that it recovers the the stochastic gradients of \mathcal{L}_{VI} by setting $\alpha = 1$ in (7) since now $w_1(\boldsymbol{\epsilon}; \phi, \mathbf{x}) = 1$, which means the resulting algorithm unifies the computation for all finite α settings. For MC approximation, we use K samples to approximately compute the weight $\hat{w}_{\alpha,k}(\boldsymbol{\epsilon}_k; \phi, \mathbf{x}) \propto \left(\frac{p(g_\phi(\boldsymbol{\epsilon}_k), \mathbf{x})}{q(g_\phi(\boldsymbol{\epsilon}_k))} \right)^{1-\alpha}$, $k = 1, \dots, K$, and the stochastic gradient becomes

$$\nabla_\phi \hat{\mathcal{L}}_{\alpha,K}(q_\phi; \mathbf{x}) = \sum_{k=1}^K \left[\hat{w}_{\alpha,k}(\boldsymbol{\epsilon}_k; \phi, \mathbf{x}) \nabla_\phi \log \frac{p(g_\phi(\boldsymbol{\epsilon}_k), \mathbf{x})}{q(g_\phi(\boldsymbol{\epsilon}_k))} \right]. \quad (8)$$

When $\alpha = 1$, $\hat{w}_{1,k}(\boldsymbol{\epsilon}_k; \phi, \mathbf{x}) = 1/K$, and it recovers the stochastic gradient VI method [15].

To speed-up learning previous authors [14] have suggested back-propagating only one sample $\boldsymbol{\epsilon}_j$ with $j \sim p_j = \hat{w}_{\alpha,j}$, which can be easily extended to our framework. Importantly, the use of different $\alpha < 1$ indicates the degree of emphasising locations where the approximation q under-estimates p , and in the extreme case $\alpha \rightarrow -\infty$, the algorithm chooses the sample that has the *maximum* unnormalised importance weight. We name this approach *VR-max* and summarise it and other finite α settings in Algorithm 1. Note that VR-max (and VR- α with $\alpha < 0$) does *not* minimise $D_{1-\alpha}[p||q]$. It is true that $\mathcal{L}_\alpha \geq \log p(\mathbf{x})$ for negative α values. However Corollary 1 suggests that the tightest MC approximation for given K

Algorithm 1 One gradient step for VR- α /VR-max with single backward pass. Here $\hat{w}(\epsilon_k; \mathbf{x})$ short-hands $\hat{w}_{0,k}(\epsilon_k; \phi, \mathbf{x})$ in the main text.

- 1: given the current datapoint \mathbf{x} , sample $\epsilon_1, \dots, \epsilon_K \sim p(\epsilon)$
- 2: for $k = 1, \dots, K$, compute the unnormalised weight

$$\log \hat{w}(\epsilon_k; \mathbf{x}) = \log p(g_{\phi}(\epsilon_k), \mathbf{x}) - \log q(g_{\phi}(\epsilon_k) | \mathbf{x})$$

- 3: choose the sample ϵ_j to back-propagate:
 - if $|\alpha| < \infty$: $j \sim p_k$ where $p_k \propto \hat{w}(\epsilon_k; \mathbf{x})^{1-\alpha}$
 - if $\alpha = -\infty$: $j = \arg \max_k \log \hat{w}(\epsilon_k; \mathbf{x})$
 - 4: return the gradients $\nabla_{\phi} \log \hat{w}(\epsilon_j; \mathbf{x})$
-

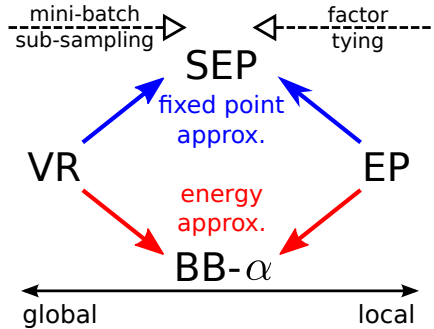


Figure 3: Connecting local and global divergence minimisation.

has non-positive α_K value. Furthermore α_K becomes more negative as the mismatch between q and p increases. This is the case for VAEs even at convergence because the uni-modal q distribution is fitted to approximate the typically multi-modal true posterior.

4.3 Stochastic approximation for large-scale learning

VR bounds can also be applied to full Bayesian inference with posterior approximation. However for large datasets full batch learning will be very inefficient. Mini-batch training is non-trivial here since the VR bound cannot be represented by the expectation of a datapoint-wise loss, except when $\alpha = 1$. This section introduces two proposals for mini-batch training, and interestingly, this recovers two existing algorithms that were motivated from a different perspective. In the following we define the ‘‘average likelihood’’ $\bar{f}_{\mathcal{D}}(\theta) = [\prod_{n=1}^N p(\mathbf{x}_n | \theta)]^{\frac{1}{N}}$. Hence the joint distribution can be rewritten as $p(\theta, \mathcal{D}) = p_0(\theta) \bar{f}_{\mathcal{D}}(\theta)^N$. Also for a mini-batch of M datapoints $\mathcal{S} = \{\mathbf{x}_{n_1}, \dots, \mathbf{x}_{n_M}\} \sim \mathcal{D}$, we define the ‘‘subset average likelihood’’ $\bar{f}_{\mathcal{S}}(\theta) = [\prod_{m=1}^M p(\mathbf{x}_{n_m} | \theta)]^{\frac{1}{M}}$.

The first proposal considers fixed point approximation with mini-batch sub-sampling. For example, if the q distribution has an exponential family form, then the gradient of \mathcal{L}_{α} w.r.t. the natural parameters of q will match the moments between $q(\theta)$ and the tilted distribution $\tilde{p}_{\alpha}(\theta) \propto q(\theta)^{\alpha} p_0(\theta)^{1-\alpha} \bar{f}_{\mathcal{D}}(\theta)^{N(1-\alpha)}$ when $\alpha \neq 1$. Now given a mini-batch of datapoints \mathcal{S} , the moment matching update can be approximated by replacing $\bar{f}_{\mathcal{D}}(\theta)$ with $\bar{f}_{\mathcal{S}}(\theta)$. The second proposal also applies this subset average likelihood approximation idea, but directly to the VR bound (10) (so this approach is named energy approximation):

$$\tilde{\mathcal{L}}_{\alpha}(q; \mathcal{S}) = \frac{1}{1-\alpha} \log \mathbb{E}_q \left[\left(\frac{p_0(\theta) \bar{f}_{\mathcal{S}}(\theta)^N}{q(\theta)} \right)^{1-\alpha} \right]. \quad (9)$$

In the appendix we demonstrate with detailed derivations that fixed point approximation returns Stochastic EP (SEP) [6], and black box alpha (BB- α) [13] correspond to energy approximation. Both algorithms were originally proposed to approximate (power) EP [3, 23], which usually considers $M = 1$ and $\alpha \in [1 - 1/N, 1)$. These approximations were done by factor tying, which significantly reduces the memory overhead of full EP and makes both SEP and BB- α scalable to large datasets just as VI. But more importantly, EP minimises α -divergence *locally*. Hence the new derivation sheds lights on the connections between *local* and *global* divergence minimisations as depicted in Figure 3. Note that all these methods recover SVI when $\alpha \rightarrow 1$, in which global and local divergence minimisation are equivalent. Also these two proposals can be viewed as extending recent attempts of distributed posterior approximation (by carving up the dataset into pieces with $M > 1$ [9, 10]) to both SEP and BB- α .

Monte Carlo methods can also be applied to both proposals. For SEP the moment computation can be approximated with MCMC [9, 10]. For BB- α one can show in the same way as to prove Theorem 2 that simple MC approximation in expectation lower-bounds the BB- α energy when $\alpha \leq 1$. In general it is also an open question how to choose α to guarantee a lower-bound to $\log p(\mathcal{D})$ for given the mini-batch size M and the number of samples K .

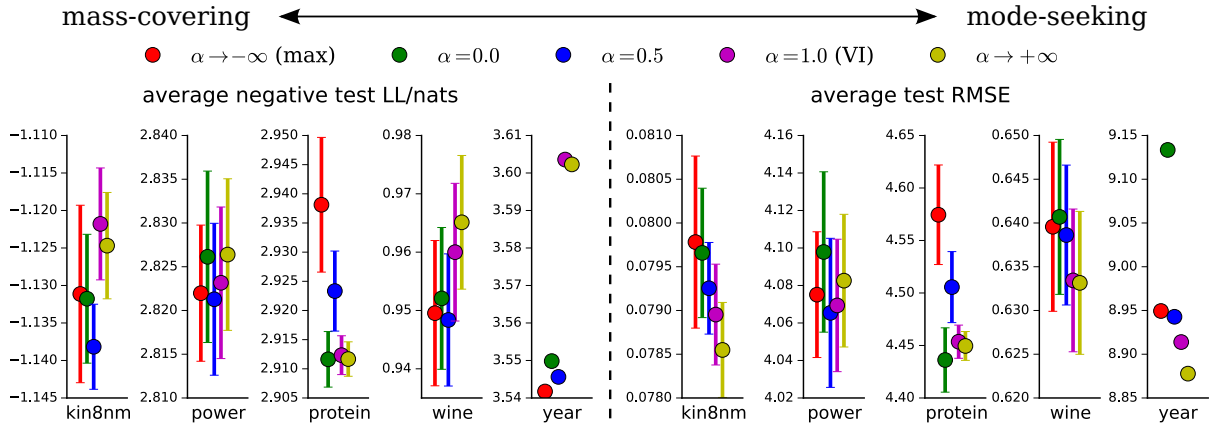


Figure 4: Test NLL and RMSE results for Bayesian neural network regression. The lower the better.

5 Experiments

We evaluated the VR bound methods on Bayesian neural networks and variational auto-encoders. Readers are referred to the appendix for detailed experimental set-up (batch size, learning rate for the ADAM optimizer [24], etc.).

5.1 Bayesian neural network

The first experiment considers Bayesian neural network regression. The datasets are collected from the UCI dataset repository.¹ The model is a single-layer neural networks with 50 hidden units (ReLUs) for all datasets except Protein and Year (100 units). We use a Gaussian prior $\theta \sim \mathcal{N}(\theta; \mathbf{0}, \mathbf{I})$ for the network weights and Gaussian approximation to the true posterior $q(\theta) = \mathcal{N}(\theta; \mu_q, \text{diag}(\sigma_q))$. We follow the toy example in Section 3 to consider $\alpha \in \{-\infty, 0.0, 0.5, 1.0, +\infty\}$ in order to examine the effect of mass-covering/mode-seeking behaviour. Stochastic optimisation uses the energy approximation proposal in Section 4.3 as the largest dataset (Year) contains more than $N = 500,000$ datapoints. MC approximation is also deployed to compute the energy function, in which $K = 100, 10$ is used for small and large datasets (Protein and Year), respectively.

We summarise the test negative log-likelihood (NLL) and RSME with standard error (across different random splits except for Year) for selected datasets in Figure 4, where the full results are provided in the appendix. These results indicate that for posterior approximation problems, the optimal α may vary for different datasets. Future work should develop algorithms to automatically select the best α values, although a naïve approach can use validation sets. But we still observed two major trends that, mode-seeking methods tend to focus on improving the predictive error, while mass-covering regimes calibrate the uncertainty estimate and return better test log-likelihood. In particular, VI returns lower test log-likelihood for most of the datasets. Furthermore, $\alpha = 0.5$ produced overall good results for both test NLL and RMSE, probably because the skew symmetry is centred at $\alpha = 0.5$ and the corresponding divergence is the only symmetric distance measure in the family.

5.2 Variational auto-encoder

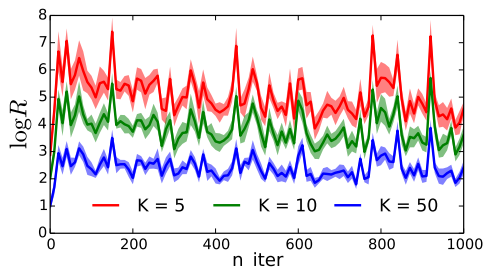
The second experiment considers variational auto-encoders for unsupervised learning. We mainly compare three approaches: VAE ($\alpha = 1.0$), IWAE ($\alpha = 0$), and VR-max ($\alpha \rightarrow -\infty$), which are implemented upon the publicly available code.² Four datasets are considered: Frey Face (with 10-fold cross validation), Caltech 101 Silhouettes, MNIST and OMNIGLOT. The VAE model has $L = 1, 2$ stochastic layers with deterministic layers stacked between, where the network architecture is detailed in the appendix. We reproduce the IWAE experiments to obtain a fair comparison, since the results in the original publication [14] does not match those evaluated on the publicly available code.

¹<http://archive.ics.uci.edu/ml/datasets.html>

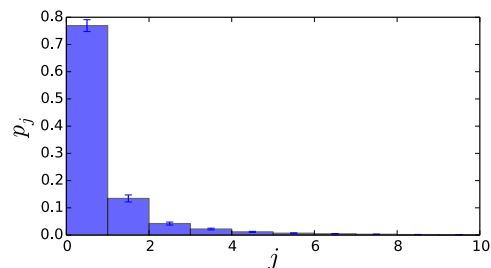
²<https://github.com/yburda/iwae>

Table 2: Average Test log-likelihood. Results for VAE on MNIST and OMNIGLOT are collected from [14]. IWAE results are reproduced using the publicly available code.

Dataset	L	K	VAE	IWAE	VR-max
Frey Face	1	5	1322.96	1380.30	1377.40
(\pm std. err.)			± 10.03	± 4.60	± 4.59
Caltech 101	1	5	-119.69	-117.89	-118.01
Silhouettes		50	-119.61	-117.21	-117.10
MNIST	1	5	-86.47	-85.41	-85.42
		50	-86.35	-84.80	-84.81
	2	5	-85.01	-83.92	-84.04
		50	-84.78	-83.05	-83.44
OMNIGLOT	1	5	-107.62	-106.30	-106.33
	1	50	-107.80	-104.68	-105.05
	2	5	106.31	-104.64	-104.71
	2	50	106.30	-103.25	-103.72



(a) Log of ratio $R = w_{max}/(1 - w_{max})$



(b) Weights of samples.

Figure 6: Importance weights during training, see main text for details. Best viewed in colour.

We report the test likelihood results in Table 2 by computing $\log p(\mathbf{x}) \approx \hat{\mathcal{L}}_{0,5000}(q; \mathbf{x})$ following [14]. We also present some samples from VR-max trained models in the appendix. Overall VR-max produces almost indistinguishable performances to IWAE on all the datasets. Other positive alpha settings (e.g. $\alpha = 0.5$) return worse results, e.g. 1374.64 ± 5.62 for Frey Face and -85.50 for MNIST with $L = 1$ and $K = 5$. These results indicate the preference of better approximations to the likelihood function for MLE problems.

VR-max’s success can be explained by the tightness of the VR bound. To evaluate this conjecture, we took the VAE trained on Frey Face data, and compute the VR bounds on 100 datapoints sampled from test data using $K = \{5, 50\}$ and non-positive alphas $\alpha \in \{0, -1, -5, -50, -500\}$. Figure 5 presents the bias values $\hat{\mathcal{L}}_{\alpha,K} - \hat{\mathcal{L}}_{0,5000}$. As expected $\hat{\mathcal{L}}_{\alpha,K}$ lower-bounds the log-likelihood, where the gap is narrowed as $\alpha \rightarrow -\infty$. Also increasing the number of samples K provides improvements. The standard error of estimation is almost constant for different α (with K fixed), and is negligible when compared to the bias of MC approximation.

Another explanation for VR-max’s success is that, the contribution of the samples is dominated by the one with the largest normalised importance weight w_{max} . This is confirmed by tracking the ratio $R = w_{max}/(1 - w_{max})$ during training on Frey Face data, shown in Figure 6(a). Also Figure 6(b) shows the 10 largest importance weights from $K = 50$ samples in descending order. Now the normalised importance weights exhibit an exponential decay behaviour, with the largest weight occupying more than 75% of the probability mass. This indicates that IWAE is inefficient as it wastes most of the computation on the samples with negligible contributions to the update. Hence single backward pass can be used to reduce the computational cost, and the VR bound theory also justifies the proposed approach that only retains the largest weight.

6 Conclusion

We have presented the variational Rényi bound and its optimisation framework. We have shown the richness of the new family, not only by connecting to existing approaches including VI/VB, SEP, BB-

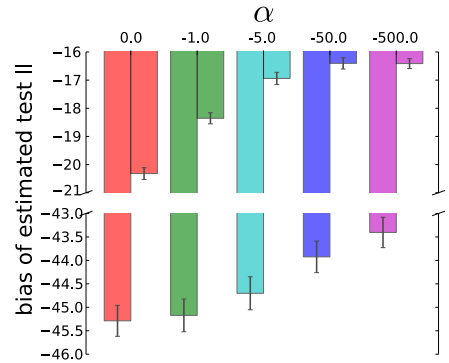


Figure 5: Bias of sampling approximation to. Results for $K = 5, 50$ samples are shown on the left and right, respectively.

α , VAE and IWAE, but also by proposing the VR-max algorithm as a new special case. Empirical results on Bayesian neural networks and variational auto-encoders indicate that VR bound methods are widely applicable and can obtain state-of-the-art results. Future work will focus on both experimental and theoretical sides. The VR bound methods should be tested on other popular probabilistic models. Theoretical work will study the interaction of the biases introduced by MC approximation and datapoint sub-sampling. Theoretical and empirical studies on choosing optimal α values will guide practitioners to using the appropriate algorithm for their applications.

References

- [1] M. I. Jordan, Z. Ghahramani, T. S. Jaakkola, and L. K. Saul, “An introduction to variational methods for graphical models,” *Machine learning*, vol. 37, no. 2, pp. 183–233, 1999.
- [2] M. J. Beal, *Variational algorithms for approximate Bayesian inference*. PhD thesis, University College London, 2003.
- [3] T. Minka, “Expectation propagation for approximate Bayesian inference,” in *Uncertainty in Artificial Intelligence*, vol. 17, pp. 362–369, 2001.
- [4] M. Opper and O. Winther, “Expectation consistent approximate inference,” *The Journal of Machine Learning Research*, vol. 6, pp. 2177–2204, 2005.
- [5] M. D. Hoffman, D. M. Blei, C. Wang, and J. W. Paisley, “Stochastic variational inference,” *Journal of Machine Learning Research*, vol. 14, no. 1, pp. 1303–1347, 2013.
- [6] Y. Li, J. M. Hernández-Lobato, and R. E. Turner, “Stochastic expectation propagation,” in *Neural Information Processing Systems*, 2015.
- [7] G. Dehaene and S. Barthelmé, “Expectation propagation in the large-data limit,” *arXiv:1503.08060*, 2015.
- [8] T. Broderick, N. Boyd, A. Wibisono, A. C. Wilson, and M. I. Jordan, “Streaming variational bayes,” in *Neural Information Processing Systems* (C. J. C. Burges, L. Bottou, Z. Ghahramani, and K. Q. Weinberger, eds.), pp. 1727–1735, 2013.
- [9] A. Gelman, A. Vehtari, P. Jylänki, C. Robert, N. Chopin, and J. P. Cunningham, “Expectation propagation as a way of life,” *arXiv:1412.4869*, 2014.
- [10] M. Xu, B. Lakshminarayanan, Y. W. Teh, J. Zhu, and B. Zhang, “Distributed bayesian posterior sampling via moment sharing,” in *Neural Information Processing Systems*, 2014.
- [11] R. Ranganath, S. Gerrish, and D. M. Blei, “Black box variational inference,” in *The 17th International Conference on Artificial Intelligence and Statistics (AISTATS)*, 2014.
- [12] A. Kucukelbir, R. Ranganath, A. Gelman, and D. M. Blei, “Automatic variational inference in stan,” in *Neural Information Processing Systems*, 2015.
- [13] J. M. Hernández-Lobato, Y. Li, M. Rowland, D. Hernández-Lobato, T. Bui, and R. E. Turner, “Black-box α -divergence minimization,” in *International Conference of Machine Learning*, 2016.
- [14] Y. Burda, R. Grosse, and R. Salakhutdinov, “Importance weighted autoencoders,” in *International Conference on Learning Representations*, 2016.
- [15] D. P. Kingma and M. Welling, “Auto-encoding variational bayes,” in *International Conference on Learning Representations*, 2014.
- [16] D. J. Rezende, S. Mohamed, and D. Wierstra, “Stochastic backpropagation and approximate inference in deep generative models,” in *International Conference of Machine Learning*, 2014.
- [17] A. Rényi, “On measures of entropy and information,” *Fourth Berkeley symposium on mathematical statistics and probability*, vol. 1, 1961.
- [18] S.-i. Amari, *Differential-Geometrical Methods in Statistic*. New York: Springer, 1985.

- [19] C. Tsallis, “Possible generalization of boltzmann-gibbs statistics,” *Journal of statistical physics*, vol. 52, no. 1-2, pp. 479–487, 1988.
- [20] T. Van Erven and P. Harremoës, “Rényi divergence and kullback-leibler divergence,” *Information Theory, IEEE Transactions on*, vol. 60, no. 7, pp. 3797–3820, 2014.
- [21] P. Grünwald, *Minimum Description Length Principle*. MIT press, Cambridge, MA, 2007.
- [22] R. E. Turner and M. Sahani, “Two problems with variational expectation maximisation for time-series models,” in *Bayesian Time series models* (D. Barber, T. Cemgil, and S. Chiappa, eds.), ch. 5, pp. 109–130, Cambridge University Press, 2011.
- [23] T. Minka, “Power EP,” Tech. Rep. MSR-TR-2004-149, Microsoft Research, Cambridge, 2004.
- [24] D. P. Kingma and J. Ba, “Adam: A method for stochastic optimization,” in *International Conference of Learning Representations*, 2015.

A Other α -divergence definitions

Here we include some existing α -divergence definitions other than Rényi's.

- Amari's α -divergence [18]

$$D_\alpha[p||q] = \frac{4}{1-\alpha^2} \left(1 - \int p(\boldsymbol{\theta})^{\frac{1+\alpha}{2}} q(\boldsymbol{\theta})^{\frac{1-\alpha}{2}} d\boldsymbol{\theta} \right).$$

- Tsallis's α -divergence [19]

$$D_\alpha[p||q] = \frac{1}{\alpha-1} \left(\int p(\boldsymbol{\theta})^\alpha q(\boldsymbol{\theta})^{1-\alpha} d\boldsymbol{\theta} - 1 \right).$$

Consider the problem of posterior approximation by minimising an α -divergence. When the approximate posterior q has an exponential family form, minimising $D_\alpha[p||q]$, no matter which definition above is used (although may use different alpha), requires moment matching to the tilted distribution $\tilde{p}_\alpha(\boldsymbol{\theta}) \propto p(\boldsymbol{\theta})^\alpha q(\boldsymbol{\theta})^{1-\alpha}$. In EP literature Amari's definition is often discussed. We focus on Rényi's definition in the main text simply because $D_\alpha[q(\boldsymbol{\theta})||p(\boldsymbol{\theta}|\mathcal{D})]$ using Rényi's definition contains $\log p(\mathcal{D})$ that can be cancelled in the same way as VI is derived.

B A mean-field approximation example

We present the mean-field approximation method for the VR bound family, with Bayesian linear regression as an illustrating example. Recall the VR bound for $\alpha \neq 1$:

$$\mathcal{L}_\alpha(q; \mathcal{D}) := \frac{1}{1-\alpha} \log \mathbb{E}_q \left[\left(\frac{p(\boldsymbol{\theta}, \mathcal{D})}{q(\boldsymbol{\theta})} \right)^{1-\alpha} \right], \quad (10)$$

where the q distribution is factorised over the components of $\boldsymbol{\theta} = (\theta_1, \dots, \theta_d)$: $q(\boldsymbol{\theta}) = \prod_i q(\theta_i)$. In the following we denote $q_j = q(\theta_j)$ to reduce notational clutter, and re-write the VR bound as

$$\begin{aligned} \mathcal{L}_\alpha(q; \mathcal{D}) &= \frac{1}{1-\alpha} \log \int \prod_i q_i(\theta_i) \left(\frac{p(\boldsymbol{\theta}, \mathcal{D})}{\prod_i q_i} \right)^{1-\alpha} d\boldsymbol{\theta} \\ &= \frac{1}{1-\alpha} \log \int q_j(\theta_j)^\alpha \left(\int \prod_{i \neq j} q_i \left(\frac{p(\boldsymbol{\theta}, \mathcal{D})}{\prod_{i \neq j} q_i} \right)^{1-\alpha} d\boldsymbol{\theta}_{i \neq j} \right) d\theta_j \\ &:= \frac{1}{1-\alpha} \log \int q_j^\alpha \tilde{p}_j^{1-\alpha} d\theta_j + \text{const}, \end{aligned}$$

where \tilde{p}_j denote the ‘‘marginal’’ distribution satisfying

$$\log \tilde{p}_j = \frac{1}{1-\alpha} \log \int \prod_{i \neq j} q_i(\theta_i) \left(\frac{p(\boldsymbol{\theta}, \mathcal{D})}{\prod_{i \neq j} q_i} \right)^{1-\alpha} d\boldsymbol{\theta}_{i \neq j} + \text{const}.$$

Now maximising the VR bound (when $\alpha > 0$, and for $\alpha < 0$ we minimise the bound) is equivalent to minimising $D_\alpha[q_j||\tilde{p}_j]$ (for $\alpha > 0$, and when $\alpha < 0$ we minimise $D_{1-\alpha}[\tilde{p}_j||q_j]$), which means $\log q_j = \log \tilde{p}_j$. One can verify that when $\alpha \rightarrow 1$ it recovers the traditional variational mean-field approximation

$$\lim_{\alpha \rightarrow 1} q_j = \int \prod_{i \neq j} q_i \log p(\boldsymbol{\theta}, \mathcal{D}) d\boldsymbol{\theta}_{i \neq j} + \text{const},$$

and when $\alpha \rightarrow 0$ it returns the exact marginal of the posterior distribution $\lim_{\alpha \rightarrow 0} q_j = p(\theta_j|\mathcal{D})$.

Now consider a Bayesian linear regression with 2-D input \mathbf{x} and 1-D output y , as an example:

$$\boldsymbol{\theta} \sim \mathcal{N}(\boldsymbol{\theta}; \boldsymbol{\mu}_0, \boldsymbol{\Lambda}_0^{-1}), \quad y|\mathbf{x} \sim \mathcal{N}(y; \boldsymbol{\theta}^T \mathbf{x}, \sigma^2).$$

Given the observations $\mathcal{D} = \{\mathbf{x}_n, y_n\}$, the posterior distribution of $\boldsymbol{\theta}$ can be computed analytically as $p(\boldsymbol{\theta}|\mathcal{D}) = \mathcal{N}(\boldsymbol{\theta}; \boldsymbol{\mu}, \boldsymbol{\Lambda}^{-1})$ with $\boldsymbol{\Lambda} = \boldsymbol{\Lambda}_0 + \frac{1}{\sigma^2} \sum_n \mathbf{x}_n \mathbf{x}_n^T$ and $\boldsymbol{\Lambda}\boldsymbol{\mu} = \boldsymbol{\Lambda}_0\boldsymbol{\mu}_0 + \frac{1}{\sigma^2} \sum_n y_n \mathbf{x}_n$. To see how the mean-field approach work we explicitly write down the elements of the posterior parameters

$$\boldsymbol{\mu} = \begin{pmatrix} \mu_1 \\ \mu_2 \end{pmatrix}, \quad \boldsymbol{\Lambda} = \begin{pmatrix} \Lambda_{11} & \Lambda_{12} \\ \Lambda_{21} & \Lambda_{22} \end{pmatrix}, \quad \Lambda_{12} = \Lambda_{21},$$

and define $q_i = \mathcal{N}(\theta_i; m_i, \lambda_i^{-1})$ as univariate Gaussian distributions. Then

$$\begin{aligned} \log q_1 &= \frac{1}{1-\alpha} \log \int q_2(\theta_2) \left(\frac{p(\boldsymbol{\theta}, \mathcal{D})}{q_2} \right)^{1-\alpha} d\theta_2 + \text{const} \\ &= \frac{1}{1-\alpha} \log \int \exp \left[-\frac{1-\alpha}{2} (\boldsymbol{\theta} - \boldsymbol{\mu})^T \boldsymbol{\Lambda} (\boldsymbol{\theta} - \boldsymbol{\mu}) - \frac{\alpha}{2} \lambda_2 (\theta_2 - m_2)^2 \right] d\theta_2 + \text{const} \\ &= \frac{1}{1-\alpha} \log \int \mathcal{N}(\boldsymbol{\theta}; \tilde{\boldsymbol{\mu}}, \tilde{\boldsymbol{\Sigma}}) d\theta_2 + \text{const} \\ &= \log \mathcal{N}(\theta_1; m_1, \lambda_1^{-1}) + \text{const}, \end{aligned}$$

where the new mean m_1 and the precision λ_1 satisfies

$$\begin{aligned} m_1 &= \mu_1 + C_1(\mu_2 - m_2), \quad C_1 = \frac{\alpha \lambda_2 \Lambda_{12}}{(1-\alpha)|\boldsymbol{\Lambda}| + \alpha \lambda_2 \Lambda_{11}}, \\ \lambda_1 &= \Lambda_{11} - (1-\alpha)\Lambda_{12}((1-\alpha)\Lambda_{22} + \alpha \lambda_2)^{-1} \Lambda_{21}. \end{aligned}$$

One can derive the mean m_2 for q_2 in the same way, and show that $\mathbf{m} = \boldsymbol{\mu}$ is the only fixed point of this iterative update. So we have $q_1 = \mathcal{N}(\theta_1; \mu_1, \lambda_1^{-1})$, and similarly $q_2 = \mathcal{N}(\theta_2; \mu_2, \lambda_2^{-1})$ with $\lambda_2 = \Lambda_{22} - (1-\alpha)\Lambda_{21}((1-\alpha)\Lambda_{11} + \alpha \lambda_1)^{-1} \Lambda_{12}$. In this example λ_1, λ_2 are feasible for all α , and solving the fixed point equations, finally we have

$$\lambda_1 = \rho_\alpha \Lambda_{11}, \quad \lambda_2 = \rho_\alpha \Lambda_{22}, \quad \rho_\alpha = \frac{1}{2\alpha} \left[(2\alpha - 1) + \sqrt{1 - \frac{4\alpha(1-\alpha)\Lambda_{12}^2}{\Lambda_{11}\Lambda_{22}}} \right].$$

One can show that $\lim_{\alpha \rightarrow 1} \lambda_1 = \Lambda_{11}$, $\lim_{\alpha \rightarrow 0} \lambda_1 = \Lambda_{11} - \Lambda_{12} \Lambda_{22}^{-1} \Lambda_{21}$ and $\lim_{\alpha \rightarrow \pm\infty} \lambda_1 = \Lambda_{11} \pm |\Lambda_{12}| \sqrt{\Lambda_{11} \Lambda_{22}^{-1}}$ (similar results for λ_2). Also ρ_α is continuous and non-decreasing in α . This means one can interpolate between mass-covering and mode-seeking behaviour by increasing α values. Moreover, notice that the limiting case $\alpha \rightarrow +\infty$ still returns uncertain estimates, although it is even more over-confident than VI. This is different from maximum a posteriori (MAP) which captures the mode but only returns a point estimate.

C Proofs of the main results

We provide the proofs of the theorems presented in section 4.1 of the main text.

C.1 Proof of Theorem 2

Proof. 1) First we prove for $\alpha \leq 1$, $\mathbb{E}_{\{\mathbf{h}_k\}}[\hat{\mathcal{L}}_{\alpha, K}]$ is non-decreasing in K . It is straight forward to show the results holds for $\alpha = 1$. We follow the proof in [14] for fixed $\alpha < 1$. Let $K > 1$ and the subset of

indices $I = \{i_1, \dots, i_{K'}\} \subset \{K\}$, $K' < K$ randomly sampled from integers 1 to K . Then for any $\alpha < 1$:

$$\begin{aligned} \mathbb{E}_{\{\mathbf{h}_k\}_{k=1}^K} [\hat{\mathcal{L}}_{\alpha, K}] &= \frac{1}{1-\alpha} \mathbb{E}_{\{\mathbf{h}_k\}} \left[\log \frac{1}{K} \sum_{k=1}^K \left(\frac{p(\mathbf{h}_k, \mathbf{x})}{q(\mathbf{h}_k | \mathbf{x})} \right)^{1-\alpha} \right] \\ &= \frac{1}{1-\alpha} \mathbb{E}_{\{\mathbf{h}_k\}} \left[\log \mathbb{E}_{I \subset \{K\}} \left[\frac{1}{K'} \sum_{k=1}^K \left(\frac{p(\mathbf{h}_{i_k}, \mathbf{x})}{q(\mathbf{h}_{i_k})} \right)^{1-\alpha} \right] \right] \\ &\geq \frac{1}{1-\alpha} \mathbb{E}_{\{\mathbf{h}_k\}} \left[\mathbb{E}_{I \subset \{K\}} \left[\log \frac{1}{K'} \sum_{k=1}^K \left(\frac{p(\mathbf{h}_{i_k}, \mathbf{x})}{q(\mathbf{h}_{i_k})} \right)^{1-\alpha} \right] \right] \quad (\log x \text{ is concave}) \\ &= \frac{1}{1-\alpha} \mathbb{E}_{\{\mathbf{h}_k\}} \left[\log \frac{1}{K} \sum_{k=1}^{K'} \left(\frac{p(\mathbf{h}_k, \mathbf{x})}{q(\mathbf{h}_k | \mathbf{x})} \right)^{1-\alpha} \right] = \mathbb{E}_{\{\mathbf{h}_k\}_{k=1}^{K'}} [\hat{\mathcal{L}}_{\alpha, K'}] \end{aligned}$$

We used Jensen's inequality of logarithm for the lower-bounding result here. When $\alpha > 1$ we can prove similar result but with inequality reversed, simply because now $1 - \alpha < 0$.

2) Next we prove that, when $K \rightarrow \infty$ and $|\mathcal{L}_\alpha| < +\infty$, we have $\mathbb{E}_{\{\mathbf{h}_k\}_{k=1}^K} [\hat{\mathcal{L}}_{\alpha, K}] \rightarrow \mathcal{L}_\alpha$. We only prove it for $\alpha \leq 1$, and for $\alpha > 1$ it can be proved in a similar way. First we use Jensen's inequality again for all finite K :

$$\begin{aligned} \mathbb{E}_{\{\mathbf{h}_k\}_{k=1}^K} [\hat{\mathcal{L}}_{\alpha, K}] &= \frac{1}{1-\alpha} \mathbb{E}_{\{\mathbf{h}_k\}} \left[\log \frac{1}{K} \sum_{k=1}^K \left(\frac{p(\mathbf{h}_k, \mathbf{x})}{q(\mathbf{h}_k | \mathbf{x})} \right)^{1-\alpha} \right] \\ &\leq \frac{1}{1-\alpha} \log \mathbb{E}_{\{\mathbf{h}_k\}} \left[\frac{1}{K} \sum_{k=1}^K \left(\frac{p(\mathbf{h}_k, \mathbf{x})}{q(\mathbf{h}_k | \mathbf{x})} \right)^{1-\alpha} \right] = \mathcal{L}_\alpha. \end{aligned}$$

This implies $\limsup_{K \rightarrow +\infty} \mathbb{E}_{\{\mathbf{h}_k\}_{k=1}^K} [\hat{\mathcal{L}}_{\alpha, K}] \leq \mathcal{L}_\alpha$.

Then as an intermediate result we prove $\hat{\mathcal{L}}_{\alpha, K} \rightarrow \mathcal{L}_\alpha$ almost surely when $K \rightarrow \infty$. For $\alpha \neq 1$, since function \log is continuous we again swap the limit and logarithm:

$$\lim_{K \rightarrow +\infty} \frac{1}{1-\alpha} \log \frac{1}{K} \sum_{k=1}^K \left(\frac{p(\mathbf{h}_k, \mathbf{x})}{q(\mathbf{h}_k | \mathbf{x})} \right)^{1-\alpha} = \frac{1}{1-\alpha} \log \lim_{K \rightarrow +\infty} \frac{1}{K} \sum_{k=1}^K \left(\frac{p(\mathbf{h}_k, \mathbf{x})}{q(\mathbf{h}_k | \mathbf{x})} \right)^{1-\alpha}.$$

Now since we assume $|\mathcal{L}_\alpha| < +\infty$, this implies $\mathbb{E}_q \left[\left(\frac{p(\mathbf{h}, \mathbf{x})}{q(\mathbf{h} | \mathbf{x})} \right)^{1-\alpha} \right]$ is finite. Also notice for all α values the ratio p/q is non-negative. Thus by the strong law of large numbers we have

$$\lim_{K \rightarrow +\infty} \frac{1}{K} \sum_{k=1}^K \left(\frac{p(\mathbf{h}_k, \mathbf{x})}{q(\mathbf{h}_k | \mathbf{x})} \right)^{1-\alpha} = \mathbb{E}_{q(\mathbf{h} | \mathbf{x})} \left[\left(\frac{p(\mathbf{h}, \mathbf{x})}{q(\mathbf{h} | \mathbf{x})} \right)^{1-\alpha} \right] \text{ a. s.,}$$

then $\hat{\mathcal{L}}_{\alpha, K} \rightarrow \mathcal{L}_\alpha$ almost surely as $K \rightarrow +\infty$. When $\alpha = 1$ we can use similar method to prove $\lim_{K \rightarrow +\infty} \hat{\mathcal{L}}_{1, K} = \mathcal{L}_{VI}$ almost surely.

Finally, using the non-increasing in α property we will prove later we have $\hat{\mathcal{L}}_{\alpha, K} \geq \hat{\mathcal{L}}_{1, K}$. Thus we can apply Fatou's Lemma and obtain (notice $\mathbb{E}[\mathcal{L}_{1, K}] = \mathcal{L}_{VI}$ for all K):

$$\mathcal{L}_\alpha - \mathcal{L}_{VI} = \mathbb{E}_{\{\mathbf{h}_k\}_{k=1}^K} [\liminf_{K \rightarrow +\infty} \hat{\mathcal{L}}_{\alpha, K} - \hat{\mathcal{L}}_{1, K}] \leq \liminf_{K \rightarrow +\infty} \mathbb{E}_{\{\mathbf{h}_k\}_{k=1}^K} [\hat{\mathcal{L}}_{\alpha, K} - \hat{\mathcal{L}}_{1, K}] = \liminf_{K \rightarrow +\infty} \mathbb{E}_{\{\mathbf{h}_k\}_{k=1}^K} [\hat{\mathcal{L}}_{\alpha, K}] - \mathcal{L}_{VI}.$$

Combining with the supremum bound, we have $\mathbb{E}_{\{\mathbf{h}_k\}_{k=1}^K} [\hat{\mathcal{L}}_{\alpha, K}] \rightarrow \mathcal{L}_\alpha$ when K goes to infinity. For $\alpha < 1$ we use the non-decreasing in K property to bound the limit infimum and the non-increasing property in α to bound the limit supremum. Thus the convergence result holds for all $\alpha \in \{\alpha : |\mathcal{L}_\alpha| < +\infty\}$.

3) $\mathbb{E}[\hat{\mathcal{L}}_{\alpha, K}]$ is non-increasing in α : since expectation preserves monotonicity, it is sufficient to prove the result for $\hat{\mathcal{L}}_{\alpha, K}$. This can be proved in similar way as Theorem 3 and 39 in [20], and we include the proof here for completeness. Notice that for $\alpha < \beta$ function $x^{\frac{1-\alpha}{1-\beta}}$ defined on $x > 0$ is convex when $\alpha < 1$

and concave when $\alpha > 1$. So applying Jensen's inequality:

$$\begin{aligned}\hat{\mathcal{L}}_{\alpha,K} &= \frac{1}{1-\alpha} \log \frac{1}{K} \sum_{k=1}^K \left(\frac{p(\mathbf{h}_k, \mathbf{x})}{q(\mathbf{h}_k | \mathbf{x})} \right)^{1-\alpha} = \frac{1}{1-\alpha} \log \frac{1}{K} \sum_{k=1}^K \left(\left(\frac{p(\mathbf{h}_k, \mathbf{x})}{q(\mathbf{h}_k | \mathbf{x})} \right)^{1-\beta} \right)^{\frac{1-\alpha}{1-\beta}} \\ &\geq \frac{1}{1-\alpha} \log \left(\frac{1}{K} \sum_{k=1}^K \left(\frac{p(\mathbf{h}_k, \mathbf{x})}{q(\mathbf{h}_k | \mathbf{x})} \right)^{1-\beta} \right)^{\frac{1-\alpha}{1-\beta}} = \hat{\mathcal{L}}_{\beta,K}.\end{aligned}$$

Continuity in α : First we show $\hat{\mathcal{L}}_{\alpha,K}$ is continuous in α . For $\alpha \neq 0, 1, \infty$ and for any sequence $\{\alpha_n\} \rightarrow \alpha$ it is sufficient to show that

$$\begin{aligned}&\lim_{n \rightarrow \infty} \log \frac{1}{K} \sum_k q(\mathbf{h}_k | \mathbf{x})^{\alpha_n} p(\mathbf{h}_k, \mathbf{x})^{1-\alpha_n} \\ &= \log \lim_{n \rightarrow \infty} \frac{1}{K} \sum_k q(\mathbf{h}_k | \mathbf{x})^{\alpha_n} p(\mathbf{h}_k, \mathbf{x})^{1-\alpha_n} \quad (\log x \text{ is a continuous function}) \\ &= \log \frac{1}{K} \sum_k \lim_{n \rightarrow \infty} q(\mathbf{h}_k | \mathbf{x})^{\alpha_n} p(\mathbf{h}_k, \mathbf{x})^{1-\alpha_n} \quad (\text{finite sum}) \\ &= \log \frac{1}{K} \sum_k q(\mathbf{h}_k | \mathbf{x}) \left(\frac{p(\mathbf{h}_k, \mathbf{x})}{q(\mathbf{h}_k | \mathbf{x})} \right)^{1-\lim_{n \rightarrow \infty} \alpha_n} \quad (a^x \text{ is continuous in } x \text{ for all } a > 0) \\ &= \log \frac{1}{K} \sum_k q(\mathbf{h}_k | \mathbf{x})^\alpha p(\mathbf{h}_k, \mathbf{x})^{1-\alpha}.\end{aligned}$$

For $\alpha = 0, 1, \infty$ the Rényi divergence is defined by continuity so one can use the same technique to show the continuity of $\hat{\mathcal{L}}_{\alpha,K}$ on those α values for fixed K . Then since $\alpha_n \rightarrow \alpha$, for any $\epsilon > 0$, there exists n that is large enough such that $\alpha_m \in (\alpha - \epsilon, \alpha + \epsilon)$ for all $m > n$. Using the monotonicity result, we have for $\forall m > n$, $\hat{\mathcal{L}}_{\alpha_m,K}$ is bounded in the interval $(\hat{\mathcal{L}}_{\alpha+\epsilon,K}, \hat{\mathcal{L}}_{\alpha-\epsilon,K})$, and we can make ϵ small enough to ensure $\mathbb{E}[\hat{\mathcal{L}}_{\alpha-\epsilon,K}] < +\infty$ and $\mathbb{E}[\hat{\mathcal{L}}_{\alpha+\epsilon,K}] < +\infty$.³ This allows us to apply the dominated convergence theorem to prove $\lim_{n \rightarrow +\infty} \mathbb{E}[\hat{\mathcal{L}}_{\alpha_n,K}] = \mathbb{E}[\lim_{n \rightarrow +\infty} \hat{\mathcal{L}}_{\alpha_n,K}] = \mathbb{E}[\hat{\mathcal{L}}_{\alpha,K}]$. Thus we have proved that $\mathbb{E}[\hat{\mathcal{L}}_{\alpha,K}]$ is continuous on $\alpha \in \{|\mathcal{L}_\alpha| < +\infty\}$. \square

C.2 Proof of Corollary 1

It is sufficient to prove the corollary for the case $q(\mathbf{h} | \mathbf{x}) \neq p(\mathbf{h} | \mathbf{x})$. We first introduce the following lemma.

Lemma 1. *Assume $\alpha < 0$ and $|\mathcal{L}_\alpha| < +\infty$. Then there exists $1 \leq K_\alpha < +\infty$ such that for all $K \leq K_\alpha < K'$, $\mathbb{E}_{\{\mathbf{h}_k\}_{k=1}^K}[\hat{\mathcal{L}}_{\alpha,K}(q; \mathbf{x})] \leq \log p(\mathbf{x}) < \mathbb{E}_{\{\mathbf{h}_k\}_{k=1}^{K'}}[\hat{\mathcal{L}}_{\alpha,K'}(q; \mathbf{x})]$. Also K_α is **non-decreasing** in α with $\lim_{\alpha \rightarrow 0} K_\alpha = +\infty$ and $\lim_{\alpha \rightarrow -\infty} K_\alpha \geq 1$.*

Proof. 1) Existence of K_α : first from Theorem 2 we have $\mathbb{E}[\hat{\mathcal{L}}_{\alpha,K}]$ is non-decreasing in K when $\alpha < 0$. Then since for all α , $\mathbb{E}[\hat{\mathcal{L}}_{\alpha,1}] = \mathcal{L}_{VI} \leq \log p(\mathbf{x})$, we have $K_\alpha \geq 1$ if K_α exists. Also from Theorem 2 we have $\lim_{K \rightarrow +\infty} \mathbb{E}[\hat{\mathcal{L}}_{\alpha,K}] = \mathcal{L}_\alpha > \log p(\mathbf{x})$ for all $\alpha < 0$. Hence for $\epsilon = \mathcal{L}_\alpha - \log p(\mathbf{x})$ there exist K that is finite but large enough such that $\mathcal{L}_\alpha - \mathbb{E}[\hat{\mathcal{L}}_{\alpha,K'}] < \epsilon$ for all $K' > K$. Now we can define K_α as the minimum of such K and it is straight-forward to show that $1 \leq K_\alpha < +\infty$.

2) K_α is non-decreasing in α : suppose there exist $\alpha > \beta$ such that $K_\alpha < K_\beta$. Then there exist $K_\alpha < K \leq K_\beta$ such that $\mathbb{E}[\hat{\mathcal{L}}_{\alpha,K}] > \log p(\mathbf{x}) \geq \mathbb{E}[\hat{\mathcal{L}}_{\beta,K}]$. But Theorem 2 says $\mathbb{E}[\hat{\mathcal{L}}_{\alpha,K}]$ is non-increasing in α , a contradiction.

3) Since $\lim_{K \rightarrow +\infty} \mathbb{E}[\hat{\mathcal{L}}_{\alpha,K}] = \mathcal{L}_\alpha$ and $\mathcal{L}_\alpha \downarrow \log p(\mathbf{x})$ when $\alpha \uparrow 0$, we have $\lim_{\alpha \rightarrow 0} K_\alpha = +\infty$. Also since K_α is non-decreasing in α and is lower-bounded by 1, we have the limit exists and $\lim_{\alpha \rightarrow -\infty} K_\alpha \geq 1$. \square

Now we prove Corollary 1.

³From 2) and the monotonicity in α result, we have $\mathcal{L}_{VI} \leq \mathbb{E}[\hat{\mathcal{L}}_{\alpha,K}] \leq \mathcal{L}_\alpha$ when $\alpha \leq 1$ and $\mathcal{L}_{VI} \geq \mathbb{E}[\hat{\mathcal{L}}_{\alpha,K}] \geq \mathcal{L}_\alpha$ when $\alpha \geq 1$. Also since we assume $|\mathcal{L}_\alpha| < +\infty$ and from Proposition 1 \mathcal{L}_α is continuous in α , we can find an $\epsilon > 0$ that is small enough such that $\mathcal{L}_{\alpha-\epsilon}$ and $\mathcal{L}_{\alpha+\epsilon}$ are finite.

Proof. 1) Existence of α_K for $\lim_{\alpha \rightarrow -\infty} K_\alpha < K < +\infty$: from Lemma 1 we can find $\alpha > \beta$ such that $K_\alpha \geq K \geq K_\beta$. This means $\mathbb{E}[\hat{\mathcal{L}}_{\alpha,K}] \leq \log p(\mathbf{x}) \leq \mathbb{E}[\hat{\mathcal{L}}_{\beta,K}]$. Since $\mathbb{E}[\hat{\mathcal{L}}_{\alpha,K}]$ is continuous in α for any fixed K , there exists $\alpha \leq \gamma \leq \beta$ to have $\mathbb{E}[\hat{\mathcal{L}}_{\gamma,K}] = \log p(\mathbf{x})$. Note that γ might not be unique, so we define α_K as the minimum of such γ , which also gives $\mathbb{E}[\hat{\mathcal{L}}_{\alpha,K}] > \log p(\mathbf{x})$ for all $\alpha < \alpha_K$.

2) α_K is non-decreasing in K : suppose there exist $K < K'$ with $\alpha_K > \alpha_{K'}$. Then we can find $\alpha_K > \alpha > \alpha_{K'}$ such that $\mathbb{E}[\hat{\mathcal{L}}_{\alpha,K}] > \log p(\mathbf{x}) = \mathbb{E}[\hat{\mathcal{L}}_{\alpha_{K'},K'}] \geq \mathbb{E}[\hat{\mathcal{L}}_{\alpha,K'}]$. But from Theorem 2 $\mathbb{E}[\hat{\mathcal{L}}_{\alpha,K}]$ is non-decreasing in K , a contradiction.

3) Since $\lim_{K \rightarrow +\infty} \mathbb{E}[\hat{\mathcal{L}}_{\alpha,K}] = \mathcal{L}_\alpha$ and $\mathcal{L}_\alpha \downarrow \log p(\mathbf{x})$ when $\alpha \uparrow 0$, we have $\lim_{K \rightarrow +\infty} \alpha_K = 0$. Also for all α , $\mathbb{E}[\hat{\mathcal{L}}_{\alpha,1}] = \mathcal{L}_{VI} \leq \log p(\mathbf{x})$, so $\lim_{K \rightarrow 1} \alpha_K = -\infty$. \square

D Unified implementation: derivation details

We provide detailed derivations of the gradient computation here. Recall from the main text that when $\alpha \neq 1$, the VR bound with the reparameterisation trick becomes

$$\mathcal{L}_\alpha(q_\phi; \mathbf{x}) = \frac{1}{1-\alpha} \log \mathbb{E}_\epsilon \left[\left(\frac{p(g_\phi, \mathbf{x})}{q(g_\phi)} \right)^{1-\alpha} \right]. \quad (11)$$

So the distribution $p(\epsilon)$ does not depend on the recognition model. We short-hand $g_\phi = g_\phi(\epsilon)$, then,

$$\begin{aligned} \nabla_\phi \mathcal{L}_\alpha(q_\phi; \mathbf{x}) &= \frac{1}{1-\alpha} \nabla_\phi \log \mathbb{E}_\epsilon \left[\left(\frac{p(g_\phi, \mathbf{x})}{q(g_\phi)} \right)^{1-\alpha} \right] \\ &= \frac{1}{1-\alpha} \left(\mathbb{E}_\epsilon \left[\left(\frac{p(g_\phi, \mathbf{x})}{q(g_\phi)} \right)^{1-\alpha} \right] \right)^{-1} \mathbb{E}_\epsilon \left[\nabla_\phi \left(\frac{p(g_\phi, \mathbf{x})}{q(g_\phi)} \right)^{1-\alpha} \right] \\ &= \frac{1}{1-\alpha} \left(\mathbb{E}_\epsilon \left[\left(\frac{p(g_\phi, \mathbf{x})}{q(g_\phi)} \right)^{1-\alpha} \right] \right)^{-1} \mathbb{E}_\epsilon \left[\left(\frac{p(g_\phi, \mathbf{x})}{q(g_\phi)} \right)^{1-\alpha} \nabla_\phi (1-\alpha) \log \frac{p(g_\phi, \mathbf{x})}{q(g_\phi)} \right] \\ &= \mathbb{E}_\epsilon \left[w_\alpha(\epsilon; \phi, \mathbf{x}) \nabla_\phi \log \frac{p(g_\phi, \mathbf{x})}{q(g_\phi)} \right]. \end{aligned}$$

Here we define

$$w_\alpha(\epsilon; \phi, \mathbf{x}) := \left(\frac{p(g_\phi, \mathbf{x})}{q(g_\phi)} \right)^{1-\alpha} / \mathbb{E}_\epsilon \left[\left(\frac{p(g_\phi, \mathbf{x})}{q(g_\phi)} \right)^{1-\alpha} \right]. \quad (12)$$

For MC approximation with finite K samples, one can use the same technique to show that

$$\nabla_\phi \hat{\mathcal{L}}_{\alpha,K}(q_\phi; \mathbf{x}) = \sum_{k=1}^K \left[\hat{w}_{\alpha,k}(\epsilon_k; \phi, \mathbf{x}) \nabla_\phi \log \frac{p(g_\phi(\epsilon_k), \mathbf{x})}{q(g_\phi(\epsilon_k))} \right].$$

with the importance weights

$$\hat{w}_{\alpha,k}(\epsilon_k; \phi, \mathbf{x}) := \left(\frac{p(g_\phi(\epsilon_k), \mathbf{x})}{q(g_\phi(\epsilon_k))} \right)^{1-\alpha} / \sum_{k=1}^K \left(\frac{p(g_\phi(\epsilon_k), \mathbf{x})}{q(g_\phi(\epsilon_k))} \right)^{1-\alpha}. \quad (13)$$

One can show that $\lim_{\alpha \rightarrow 1} w_\alpha(\epsilon; \phi, \mathbf{x}) = 1$ and $\lim_{\alpha \rightarrow 1} \hat{w}_{\alpha,k}(\epsilon_k; \phi, \mathbf{x}) = 1/K$. This indicates the recovery of the original VAE algorithm.

E Stochastic approximation for large-scale learning: derivations

This section shows the connection between VR bound optimisation and the recently proposed algorithms: SEP [6] and BB- α [13], by taking $M = 1$ and $\alpha = 1 - \beta/N$.

Recall that in the main text we have defined the ‘‘average likelihood’’ $\bar{f}_{\mathcal{D}}(\theta) = [\prod_{n=1}^N p(\mathbf{x}_n|\theta)]^{\frac{1}{N}}$. Hence the joint distribution can be rewritten as $p(\theta, \mathcal{D}) = p_0(\theta) \bar{f}_{\mathcal{D}}(\theta)^N$. Also for a mini-batch of M datapoints

$\mathcal{S} = \{\mathbf{x}_{n_1}, \dots, \mathbf{x}_{n_M}\} \sim \mathcal{D}$, we define the ‘‘subset average likelihood’’ $\bar{f}_{\mathcal{S}}(\boldsymbol{\theta}) = [\prod_{m=1}^M p(\mathbf{x}_{n_m}|\boldsymbol{\theta})]^{\frac{1}{M}}$. When $M = 1$ we also write $\bar{f}_{\mathcal{S}}(\boldsymbol{\theta}) = f_n(\boldsymbol{\theta})$ for $\mathcal{S} = \{\mathbf{x}_n\}$. Now assume the posterior approximation is defined as $q(\boldsymbol{\theta}) = \frac{1}{Z_q} p_0(\boldsymbol{\theta}) t(\boldsymbol{\theta})^N$. Often $t(\boldsymbol{\theta})$ is chose to have an exponential family form $t(\boldsymbol{\theta}) \propto \exp[\langle \boldsymbol{\lambda}, \boldsymbol{\Phi}(\boldsymbol{\theta}) \rangle]$ with $\boldsymbol{\Phi}(\boldsymbol{\theta})$ denoting the sufficient statistic. Then picking $\alpha = 1 - \beta/N$, $\beta \neq 0$, we have the exact VR bound as

$$\mathcal{L}_{\alpha}(q; \mathcal{D}) = \log Z_q + \frac{N}{\beta} \log \mathbb{E}_q \left[\left(\frac{\bar{f}_{\mathcal{D}}(\boldsymbol{\theta})}{t(\boldsymbol{\theta})} \right)^{\beta} \right] \quad (14)$$

The first proposal considers deriving the fixed point conditions, then approximating them with mini-batch sub-sampling. In our example the fixed point condition for the variational parameters $\boldsymbol{\lambda}$ is

$$\nabla_{\boldsymbol{\lambda}} \mathcal{L}_{\alpha}(q; \mathcal{D}) = 0 \quad \Rightarrow \quad \mathbb{E}_q[\boldsymbol{\Phi}(\boldsymbol{\theta})] = \mathbb{E}_{\tilde{p}_{\alpha}}[\boldsymbol{\Phi}(\boldsymbol{\theta})], \quad (15)$$

with the tilted distribution defined as

$$\tilde{p}_{\alpha}(\boldsymbol{\theta}) \propto q(\boldsymbol{\theta})^{\alpha} p_0(\boldsymbol{\theta})^{1-\alpha} \bar{f}_{\mathcal{D}}(\boldsymbol{\theta})^{N(1-\alpha)} \propto p_0(\boldsymbol{\theta}) t(\boldsymbol{\theta})^{N-\beta} \bar{f}_{\mathcal{D}}(\boldsymbol{\theta})^{\beta}.$$

Now given a mini-batch of datapoints \mathcal{S} , the moment matching update can be approximated by replacing $\bar{f}_{\mathcal{D}}(\boldsymbol{\theta})$ with $\bar{f}_{\mathcal{S}}(\boldsymbol{\theta}) = [\prod_{m=1}^M p(\mathbf{x}_{n_m}|\boldsymbol{\theta})]^{\frac{1}{M}}$. More precisely, each iteration we sample a subset of data $\mathcal{S} = \{\mathbf{x}_{n_1}, \dots, \mathbf{x}_{n_M}\} \sim \mathcal{D}$, and compute the new update for $\boldsymbol{\lambda}$ by first computing $\tilde{p}_{\alpha, \mathcal{S}}(\boldsymbol{\theta}) \propto p_0(\boldsymbol{\theta}) t(\boldsymbol{\theta})^{N-\beta} \bar{f}_{\mathcal{S}}(\boldsymbol{\theta})^{\beta}$ then taking $\mathbb{E}_q[\boldsymbol{\Phi}(\boldsymbol{\theta})] \leftarrow \mathbb{E}_{\tilde{p}_{\alpha, \mathcal{S}}}[\boldsymbol{\Phi}(\boldsymbol{\theta})]$. This method returns SEP when $M = 1$, i.e. in each iteration only one datapoint is sampled to update the approximate posterior.

The second proposal also applies this subset average likelihood approximation idea, but directly to the VR bound (14), with $\mathbb{E}_{\mathcal{S}}$ denotes the expectation over mini-batch sub-sampling:

$$\mathbb{E}_{\mathcal{S}} \left[\tilde{\mathcal{L}}_{\alpha}(q; \mathcal{S}) \right] = \log Z_q + \frac{N}{\beta} \mathbb{E}_{\mathcal{S}} \left[\log \mathbb{E}_q \left[\left(\frac{\bar{f}_{\mathcal{S}}(\boldsymbol{\theta})}{t(\boldsymbol{\theta})} \right)^{\beta} \right] \right]. \quad (16)$$

It recovers the energy function of BB- α when $M = 1$. Note that the original paper [13] uses an adapted form of Amari’s α -divergence, and the α value in the BB- α algorithm corresponds to β in our exposition. Now the gradient of this approximated energy function becomes

$$\nabla_{\boldsymbol{\lambda}} \mathbb{E}_{\mathcal{S}} \left[\tilde{\mathcal{L}}_{\alpha}(q; \mathcal{S}) \right] = N(\mathbb{E}_q[\boldsymbol{\Phi}(\boldsymbol{\theta})] - \mathbb{E}_{\mathcal{S}} \mathbb{E}_{\tilde{p}_{\alpha, \mathcal{S}}}[\boldsymbol{\Phi}(\boldsymbol{\theta})]). \quad (17)$$

Both SEP and BB- α return SVI when $\alpha \rightarrow 1$ (or equivalently $\beta \rightarrow 0$). But for other α values it is important to note that these two proposals return different optimum at convergence. BB- α requires averaging the moment of the tilted distribution $\mathbb{E}_{\mathcal{S}} \mathbb{E}_{\tilde{p}_{\alpha, \mathcal{S}}}[\boldsymbol{\Phi}(\boldsymbol{\theta})]$. However SEP in expectation first computes the inverse mapping from the moment $\mathbb{E}_{\tilde{p}_{\alpha, \mathcal{S}}}[\boldsymbol{\Phi}(\boldsymbol{\theta})]$ to obtain the natural parameters $\boldsymbol{\lambda}_{\mathcal{S}}$, then updates the q distribution by $\boldsymbol{\lambda} \leftarrow \mathbb{E}_{\mathcal{S}}[\boldsymbol{\lambda}_{\mathcal{S}}]$. In general the inverse mapping is non-linear so the fixed point conditions of SEP and BB- α are different.

SEP is arguably more well justified since it returns the true posterior if the approximation family \mathcal{Q} is large enough to include the correct solution, just like VI and VR computed on the whole dataset. BB- α might still be biased even in this scenario. But BB- α is much simpler to implement since the energy function can be optimised with stochastic gradient descent. Indeed the authors of [13] considered the same black-box approach as to VI, by computing a stochastic estimate of the energy function then using automatic differentiation tools to obtain the gradients.

We also provide a bound of the energy approximation (16) by the following theorem.

Theorem 3. *If the approximate distribution $q(\boldsymbol{\theta})$ is Gaussian $\mathcal{N}(\boldsymbol{\mu}, \boldsymbol{\Sigma})$, and the likelihood functions has an exponential family form $p(\mathbf{x}|\boldsymbol{\theta}) = \exp[\langle \boldsymbol{\theta}, \boldsymbol{\Psi}(\mathbf{x}) \rangle - A(\boldsymbol{\theta})]$, then for $\alpha \leq 1$ and $r > 1$ the stochastic approximation is bounded by*

$$\mathbb{E}_{\mathcal{S}}[\tilde{\mathcal{L}}_{\alpha}(q; \mathcal{S})] \leq \mathcal{L}_{1-(1-\alpha)r}(q; \mathcal{D}) + \frac{N^2(1-\alpha)r}{2(r-1)} \text{tr}(\boldsymbol{\Sigma} \text{Cov}_{\mathcal{S} \sim \mathcal{D}}(\bar{\boldsymbol{\Psi}}_{\mathcal{S}})).$$

Proof. We substitute the exponential family likelihood term into the stochastic approximation of the VR

bound with $\alpha < 1$, and use Hölder’s inequality for any $1/r + 1/s = 1$, $r > 1$ (define $\tilde{\alpha} = 1 - (1 - \alpha)r$):

$$\begin{aligned}\mathbb{E}_{\mathcal{S}}[\tilde{\mathcal{L}}_{\alpha}(q; \mathcal{S})] &= \frac{1}{1 - \alpha} \log \mathbb{E}_q \left[\left(\frac{p_0(\boldsymbol{\theta}) \bar{f}_{\mathcal{D}}(\boldsymbol{\theta})^N \bar{f}_{\mathcal{S}}(\boldsymbol{\theta})^N}{q(\boldsymbol{\theta}) \bar{f}_{\mathcal{D}}(\boldsymbol{\theta})^N} \right)^{1 - \alpha} \right] \\ &\leq \mathcal{L}_{\tilde{\alpha}}(q; \mathcal{D}) + \frac{1}{(1 - \alpha)s} \mathbb{E}_{\mathcal{S}} \left\{ \log \mathbb{E}_q [\exp[N(1 - \alpha)s(\bar{\Psi}_{\mathcal{S}} - \bar{\Psi}_{\mathcal{D}}, \boldsymbol{\theta})]] \right\} \\ &= \mathcal{L}_{\tilde{\alpha}}(q; \mathcal{D}) + \frac{1}{(1 - \alpha)s} \mathbb{E}_{\mathcal{S}} [K_{\boldsymbol{\theta}}(N(1 - \alpha)s(\bar{\Psi}_{\mathcal{S}} - \bar{\Psi}_{\mathcal{D}}))],\end{aligned}$$

where $\bar{\Psi}_{\mathcal{S}}$ and $\bar{\Psi}_{\mathcal{D}}$ denote the mean of the sufficient statistic $\boldsymbol{\Psi}(\mathbf{x})$ on the minibatch \mathcal{S} and the whole dataset \mathcal{D} , respectively. For Gaussian distribution $q(\boldsymbol{\theta}) = \mathcal{N}(\boldsymbol{\mu}, \boldsymbol{\Sigma})$ the cumulant generating function $K_{\boldsymbol{\theta}}(\mathbf{t})$ has a closed form

$$K_{\boldsymbol{\theta}}(\mathbf{t}) = \boldsymbol{\mu}^T \mathbf{t} + \frac{1}{2} \mathbf{t}^T \boldsymbol{\Sigma} \mathbf{t}.$$

Define $\mathbf{t}_{\mathcal{S}} = N(1 - \alpha)s\Delta_{\mathcal{S}}$ with $\Delta_{\mathcal{S}} = \bar{\Psi}_{\mathcal{S}} - \bar{\Psi}_{\mathcal{D}}$, then $\mathbb{E}_{\mathcal{S}}[\mathbf{t}_{\mathcal{S}}] = \mathbf{0}$ and the upper-bound becomes

$$\begin{aligned}\mathbb{E}_{\mathcal{S}}[\tilde{\mathcal{L}}_{\alpha}(q; \mathcal{S})] &\leq \mathcal{L}_{\tilde{\alpha}}(q; \mathcal{D}) + \frac{1}{(1 - \alpha)s} \mathbb{E}_{\mathcal{S}} [K_{\boldsymbol{\theta}}(\mathbf{t}_{\mathcal{S}})] \\ &= \mathcal{L}_{\tilde{\alpha}}(q; \mathcal{D}) + \frac{1}{(1 - \alpha)s} \mathbb{E}_{\mathcal{S}} [\boldsymbol{\mu}^T \mathbf{t}_{\mathcal{S}} + \frac{1}{2} \mathbf{t}_{\mathcal{S}}^T \boldsymbol{\Sigma} \mathbf{t}_{\mathcal{S}}] \\ &= \mathcal{L}_{\tilde{\alpha}}(q; \mathcal{D}) + \frac{N^2(1 - \alpha)s}{2} \mathbb{E}_{\mathcal{S}} [\Delta_{\mathcal{S}}^T \boldsymbol{\Sigma} \Delta_{\mathcal{S}}] \\ &= \mathcal{L}_{\tilde{\alpha}}(q; \mathcal{D}) + \frac{N^2(1 - \alpha)s}{2} \text{tr}(\boldsymbol{\Sigma} \text{Cov}_{\mathcal{S} \sim \mathcal{D}}(\bar{\Psi}_{\mathcal{S}})).\end{aligned}$$

Applying the condition of Hölder’s inequality $1/r + 1/s = 1$ proves the result. \square

The following corollary is a direct result of Theorem 3 applied to BB- α . Note here we follow the convention of the original paper [13] to use $M = 1$ and denote $\alpha = \beta$ and $\mathcal{L}_{BB-\alpha}(q; \mathcal{D}) = \mathbb{E}_{\mathcal{S}} [\tilde{\mathcal{L}}_{1-\alpha/N}(q; \mathcal{S})]$.

Corollary 2. *Assume the approximate posterior and the likelihood functions satisfy the assumptions in Theorem 3, then for $\alpha > 0$ and $r > 1$, the black-box alpha energy function is upper-bounded by*

$$\mathcal{L}_{BB-\alpha}(q; \mathcal{D}) \leq \mathcal{L}_{1-\frac{\alpha r}{N}}(q; \mathcal{D}) + \frac{N\alpha r}{2(r - 1)} \text{tr}(\boldsymbol{\Sigma} \text{Cov}_{\mathcal{D}}(\boldsymbol{\Psi})).$$

F Further Experimental Details and Results

F.1 Bayesian neural network

In this section we detail the experimental set-up of the Bayesian neural network example in the main text. The likelihood function is defined as $p(y|\mathbf{x}, \boldsymbol{\theta}) = \mathcal{N}(y; F_{\boldsymbol{\theta}}(\mathbf{x}), \sigma^2)$ where $F_{\boldsymbol{\theta}}(\mathbf{x})$ denotes the non-linear transform from the neural network with weights $\boldsymbol{\theta}$. We use unit Gaussian prior $\boldsymbol{\theta} \sim \mathcal{N}(\boldsymbol{\theta}; \mathbf{0}, \mathbf{I})$ and Gaussian approximation $q(\boldsymbol{\theta}) = \mathcal{N}(\boldsymbol{\theta}; \boldsymbol{\mu}_q, \text{diag}(\boldsymbol{\sigma}_q))$, and we fit the parameters of q and the noise level σ by optimising the lower-bound. For all datasets we use single-layer neural networks with 50 hidden units (ReLUs) for datasets except Protein and Year (100 units). The methods for comparison are run for 500 iterations on the small datasets and 100, 40 iterations for the large datasets Protein and Year, respectively. We use ADAM [24] for optimisation with learning rate 0.001 and the standard setting for other parameters. For stochastic optimisation we use minibatch size $M = 32$ and number of samples $K = 100, 10$ for small and large datasets. The number of dataset random splits is 20 except for the large datasets, which is 5 and 1 for Protein and Year, respectively.

The full test results are provided in Figure 7 and Table 3, 4. In the tables the best performing results are underlined, while the worst cases are also bold-faced. Clearly the optimal α setting is dataset dependent, although for Boston and Power the performances are very similar. Also for Naval mass-covering seems to be harmful not only for predictive error but also for test log-likelihood measure. But overall mode-seeking methods tend to focus on improving the predictive error, while mass-covering regimes often return better test log-likelihood.

F.2 Variational auto-encoder

We describe the experimental set-up for the VAE experiments. The number of stochastic layers L , number of hidden units, and the activation function are summarised in Table 5. The prefix of the number indicates whether this layer is **d**eterministic or **s**tochastic, e.g. d500-s200 stands for a neural network with one deterministic layer of 500 units followed by a stochastic layer of 200 units. For Frey Face data we trained the models using learning rate 0.0005 and mini-batch size 100. For MNIST and OMNIGLOT we reused the settings from [14]: the training process ran for 3^i passes with learning rate $0.0001 \cdot 10^{-i/7}$ for $i = 0, \dots, 7$, and the batch size was 20. For Caltech Silhouettes we used the same settings as MNIST and OMNIGLOT except that the training proceeded for $\sum_{i=0}^7 2^i = 255$ iterations.

We also present some samples from the VR-max trained auto-encoders in Figure 8, and note that the visual quality of VR-max’s samples are almost identical to those from IWAE.

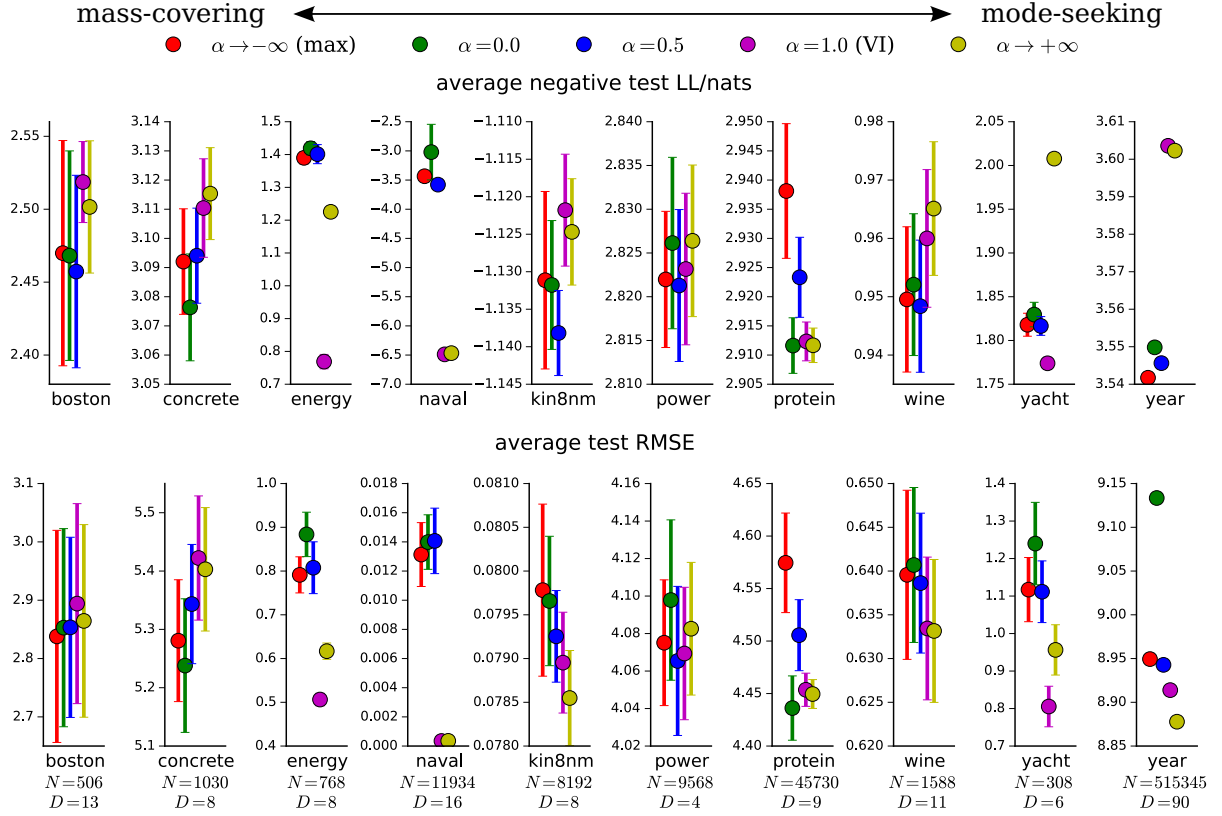


Figure 7: Test LL and RMSE results for Bayesian neural network regression. The lower the better.

Table 3: Regression experiment: Average negative test log likelihood/nats

Dataset	N	D	$\alpha \rightarrow -\infty$	$\alpha = 0.0$	$\alpha = 0.5$	$\alpha = 1.0$ (VI)	$\alpha \rightarrow +\infty$
boston	506	13	2.47±0.08	2.47±0.07	<u>2.46±0.07</u>	2.52±0.03	2.50±0.05
concrete	1030	8	3.09±0.02	<u>3.08±0.02</u>	3.09±0.02	3.11±0.02	3.12±0.02
energy	768	8	1.39±0.02	1.42±0.02	1.40±0.03	<u>0.77±0.02</u>	1.23±0.01
naval	11934	16	-3.43±0.08	-3.02±0.48	-3.58±0.08	<u>-6.49±0.04</u>	-6.47±0.09
kin8nm	8192	8	-1.13±0.01	-1.13±0.01	<u>-1.14±0.01</u>	-1.12±0.01	-1.12±0.01
power	9568	4	2.82±0.01	2.83±0.01	<u>2.82±0.01</u>	2.82±0.01	2.83±0.01
protein	45730	9	2.94±0.01	<u>2.91±0.00</u>	2.92±0.01	2.91±0.00	2.91±0.00
wine	1588	11	0.95±0.01	0.95±0.01	<u>0.95±0.01</u>	0.96±0.01	0.97±0.01
yacht	308	6	1.82±0.01	1.83±0.01	1.82±0.01	<u>1.77±0.01</u>	2.01±0.00
year	515345	90	3.54±NA	3.55±NA	3.55±NA	3.60±NA	3.60±NA
Average Rank			2.80±0.34	3.00±0.45	2.20±0.37	3.20±0.51	3.80±0.39

Table 4: Regression experiment: Average test RMSE

Dataset	N	D	$\alpha \rightarrow -\infty$	$\alpha = 0.0$	$\alpha = 0.5$	$\alpha = 1.0$ (VI)	$\alpha \rightarrow +\infty$
boston	506	13	<u>2.84±0.18</u>	2.85±0.17	2.85±0.15	2.89±0.17	2.86±0.17
concrete	1030	8	5.28±0.10	<u>5.24±0.11</u>	5.34±0.10	5.42±0.11	5.40±0.11
energy	768	8	0.79±0.04	0.88±0.05	0.81±0.06	<u>0.51±0.01</u>	0.62±0.02
naval	11934	16	0.01±0.00	0.01±0.00	0.01±0.00	<u>0.00±0.00</u>	0.00±0.00
kin8nm	8192	8	0.08±0.00	0.08±0.00	0.08±0.00	0.08±0.00	<u>0.08±0.00</u>
power	9568	4	4.08±0.03	4.10±0.04	<u>4.07±0.04</u>	4.07±0.04	4.08±0.04
protein	45730	9	4.57±0.05	<u>4.44±0.03</u>	4.51±0.03	4.45±0.02	4.45±0.01
wine	1588	11	0.64±0.01	0.64±0.01	0.64±0.01	0.63±0.01	<u>0.63±0.01</u>
yacht	308	6	1.12±0.09	1.24±0.11	1.11±0.08	<u>0.81±0.05</u>	0.96±0.07
year	515345	90	8.95±NA	9.13±NA	8.94±NA	8.91±NA	<u>8.88±NA</u>
Average Rank			3.40±0.38	3.70±0.51	3.20±0.31	2.40±0.45	2.30±0.38

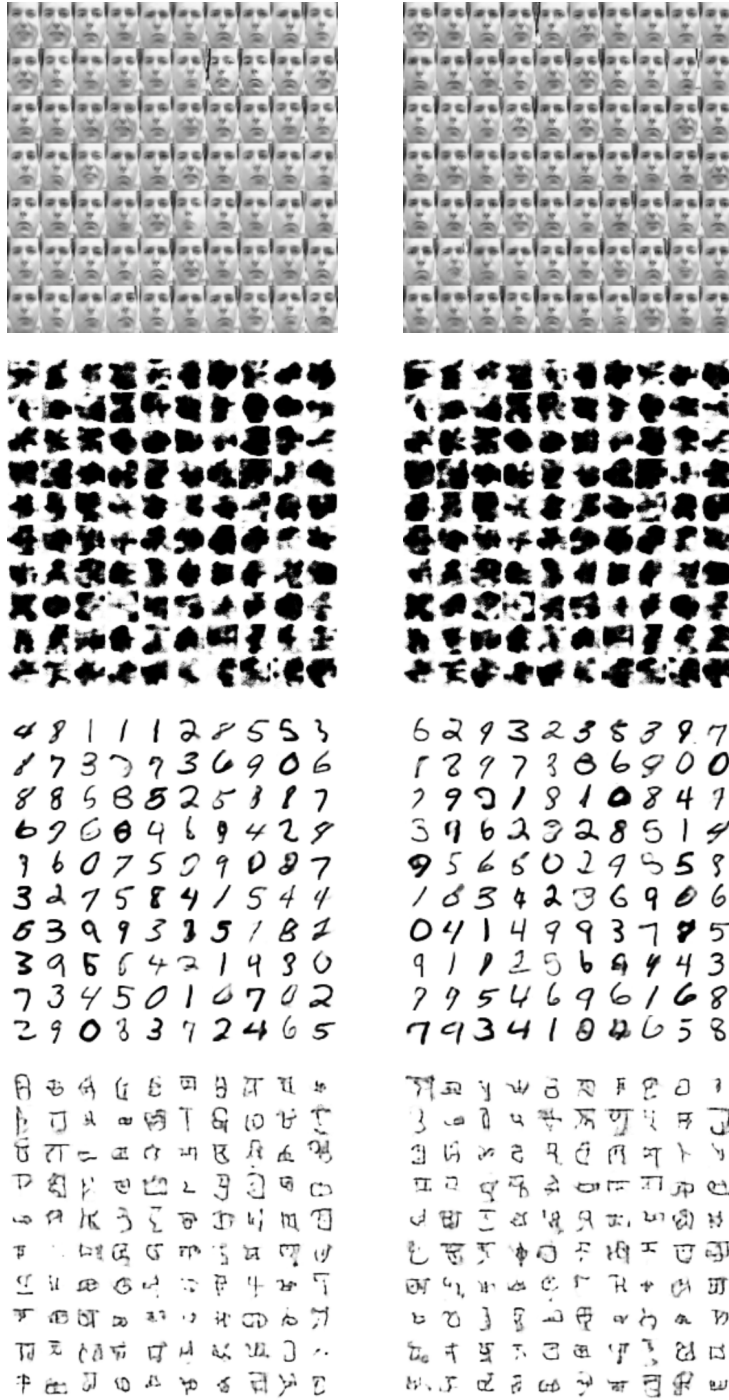


Figure 8: Sampled images from the the best models trained with IWAE (left) and VR-max (right).

Table 5: Network architecture of tested VAE algorithms.

Dataset	L	architecture	activation	probability type (p/q)
Frey Face	1	d200-d200-s20	softplus	Gaussian/Gaussian
Caltech 101	1	d500-s200	tanh	Bernoulli/Gaussian
MNIST &	1	d200-d200-s50	tanh	Bernoulli/Gaussian
OMNIGLOT	2	d200-d200-s100-d100-d100-s50	tanh	Bernoulli/Gaussian